ELECTROSPUN NANOFIBERS WITH CHEMOTACTIC CONCENTRATION GRADIENT FOR TISSUE ENGINEERING APPLICATIONS

HANDARMIN

School of Chemical and Biomedical Engineering

A thesis submitted to the Nanyang Technological University
in fulfillment of the requirement for the degree of
Master of Engineering

2011

Acknowledgment

This thesis is truly a collective effort. I am a blessed recipient of so much generous help and support from so many people. Surely, without them this thesis would not have materialized.

Foremost, I would like to convey my sincerest gratitude to none other than my supervisor, Dr. Chew Sing Yian. She has been a very supportive mentor from the very beginning. She has always been forbearing, accessible, and willing to go hands-on. I am especially grateful for the flexibility she had given me in doing my experiments, exercising my approach, and developing my own thinking all along. This has made my research life much more challenging and allowed me to learn a lot more than simply acquiring knowledge. Simply said, one honestly could not ask for better supervisor.

I benefit most from many conversations and discussions with my colleagues and fellow students. They are great and not reluctant in sharing many of their works and views. Specifically, I would like to thank Ms. Cao Haoqing for showing me how to electrospin and do SEM for the first time, Dr. Bibekananda Sundaray for the coaxial electrospinning. And also to Ms. Liu Ting, Dr. Shi Liya, Mr. Jiang Xu, Mr. Lu Jianbing, Dr. Pim-on Rujitanaroj, Ms. Low Wei ching, and Dr. Winifred Yau for so many other innumerable things. Thanks for all the knowledge that all of you have been so willingly let me steal.

I am also much indebted to the collaborators for providing me the resources, suggestion, and criticism for my work. There are many trials that would have not been possible without their generosity. Though not all is successful, I too learned so much from failure and it is just as much valuable.

I would also like to extend my gratitude to Dr. Yu Shu Chong, Ms. Myat Thiri Maw, and Dr. Wang Xiujuan for their help with confocal microscope and SEM. I have to thank Ms. Zhou Xiaojia and Mdm. Tan Lay Yen as well for helping me with procurement, paperwork, and a number of other things that made my daily research life a little bit easier. And to Mr. Chow Wai Hoong and Mr. Lim Ben Chong for their help in fabricating many custom-made items for my experiments.

Beyond research life, I wish to thanks many of my friends for all the emotional support and encouragement during difficult times. Life would certainly be harder and plain without all of you.

Lastly, I wish to express my deepest gratitude to my parents for their unwavering love. They always support me in everyway they could no matter what path I am taking.

Abstract

Engineered tissue acts as temporary construct that will be gradually replaced as the cells populate and remodel their own surrounding matrix. Laden with various cues, extracellular matrix (ECM) is cell-instructive in nature. The crosstalk between cells and ECM is, however, complex and still not emulated well by artificial scaffold due to the challenges in conferring the whole spectrum of cues. One of the challenges is to bestow chemotactic concentration gradient to implantable scaffold. The benefit is clear as cells naturally use chemotactic concentration gradient as guidance in migration and other directional processes such as neurite outgrowth. It has therefore become the aim of this project to bring this underutilized powerful factor into biomimetic electrospun fibers. We have established the methods of incorporating concentration gradient of nerve growth factor (NGF), as an example, into poly(e-caprolactone)-poly(ethylene glycol) nanofibers by coaxial electrospinning. The existence of the gradient was verified qualitatively and quantitatively. Furthermore, we demonstrated the cytocompatibility of the scaffold, released NGF bioactivity, and cellular response to the encapsulated NGF concentration gradient with PC12 cells.

In contrast to the use of synthetic polymers, harnessing the benefits of natural materials is more difficult. Lack of appropriate crosslinking technique for these hydrogel materials that could support endowed chemotactic cues necessitates the development of a new method. In attempt to address this issue, we directly encapsulated microbial transglutaminase (mTG) enzyme into electrospun gelatin fibers. The enzyme retained its catalytic capability, at least partially. We have also identified key crosslinking condition that allows the structure of majority the fibers to be preserved at physiological condition for prolonged period. Although the result is

encouraging, it is still not suitable yet to have chemotactic concentration gradient implemented. In summary, we have successfully incorporated chemotactic concentration gradient into implantable electrospun nanofibrous scaffold and developed a promising novel method of crosslinking gelatin electrospun fibers by using mTG.

Table of Contents

List of Figures and Tables

1 Introduction

1.1 Motivation

Loss of function of organ or tissue due to various causes such as accidents is often unavoidable. Even though the body has inherent albeit limited regeneration capability, this commonly leads to debilitating condition. In restricted cases, allotransplantation and xenotransplantation are still the gold standard in remediating the situation. Nevertheless, both options greatly suffer from limited supply, potential morbidity at donor site and especially for the latter; it may be further exacerbated by adverse immunorejection. Such concerns urge the search for other source of replacement tissue or organ. Growing new tissue or organ, once perceived as an inconceivable idea, is a particularly attractive and intuitive alternative. Tissue engineering, with its current state of development, has promisingly demonstrated the feasibility of such idea.

In tissue engineering, to engineer an artificial tissue construct that perfectly replicates the performance and functionality of native tissue is the ultimate goal. In practice, tissue engineering is interdisciplinary, drawing and mashing up knowledge from other related fields, such as materials science, scaffold design and fabrication, and cell biology. Although the monumental advance in relevant fields in the last few decades have helped in yielding various ways of fabricating engineered scaffolds, there is yet no ideal formulation or method of producing the perfect replica.

The main challenge lies on the dauntingly complex dynamic interaction between cells and their surrounding. Although this has been under progressively intense research, the mechanism underlying how cells perceive and translate these cues,

individually and in conjunction with others, is still largely unascertained. Cells are indispensable main biological building block and their surrounding environment provides myriad of extracellular cues that governs cellular fate and function. These cues come from many physical and chemical facets of extracellular matrix (ECM) such as topographical feature, mechanical properties, cell-cell interaction, presence of both bound and soluble bioactive chemical and their distribution in varying time and space.

In recent years, wealth of research has established that ECM assumes more functions rather just being a mere anchor or support structure. This riveting finding has in fact fostered the design philosophy that centered on mimicking the native ECM of interest. Another equally important concept is the availability of certain bioactive chemicals such as growth factors and cytokines that promotes beneficial action. Such notion has been ubiquitous in implementation through encapsulation and release of bioactive chemicals in sustained manner over prolonged period. Not only restricted to those bioactive chemicals typically secreted by cells, synthetic drugs, and genes (RNA and DNA) have also been successfully incorporated and delivered. The least often mentioned and explored is probably spatial distribution of bioactive chemicals in the form of concentration gradient. These concentration gradient, both of substrate bound and diffusible molecules, provides directed cues associated with many cellular functions such as cell movement and migration, and directed cellular projection like neurite outgrowth.

In engineering the scaffold it is important to multiple design aspects such as material, mechanical properties, architecture, and delivery of bioactive chemicals, into consideration. However concentration gradient, more often than not, is an exception despite its robust prowess. Lack of reliable method of integrating concentration

gradient into implantable scaffold, with chemotactic concentration gradient in particular, is the major hurdle.

From many established fabrication methods, fibrous scaffold made by electrospinning has received much interest in recent years. The ability to produce fibers in similar scale as ECM's fibrillar components is the most focal advantage among many others. *T*ogether with wide range of materials that can be processed and its flexibility, electrospinning is chosen as the fabrication method in this project. Providing chemotactic concentration gradient for extended period requires the encapsulated bioactive chemicals to be released in sustained manner. This prerequisite is another important consideration in establishing the incorporation method apart from the method to confer the gradient.

Natural and synthetic biomaterials have their own advantages and disadvantages in their implementation. Given the inherently different properties, the approach taken to integrate the concentration gradient may be different. While synthetic materials are easier to electrospin, natural materials typically offer much superior bio and cytocompatibility. These natural materials however need to be crosslinked in order to increase their mechanical properties and decrease their solubility in water. Though there are a few methods of crosslinking electrospun fibers, none are deemed to be ideal in attempt to impart diffusible bioactive chemicals or chemotactic concentration gradient. To prevent significant lost of encapsulated concentration gradient, it is important to have the crosslinking done *in situ* or in the absence of liquid medium. Concerns about toxicity and efficacy of the crosslinking procedures are other significant drawbacks of currently available techniques. Hence for natural materials, it is essential to first find an appropriate *in situ* crosslinking method without incurring toxicity to cells.

1.2 Objectives

The purpose of this project is to explore the feasibility of incorporating concentration gradient of bioactive chemicals into electrospun fibers, both made of natural materials and synthetic materials. Since crosslinking is of great consequence in the effort of endowing chemotactic concentration gradient to natural materials, the development of new method to overcome the limitations inflicted by current practices is imperative. We have identified such potential method. A preliminary and qualitative study investigating the method was conducted before deciding whether the concentration gradient can be imparted subsequently. In particular, there are two specific aims.

The first specific aim of the project is to investigate the electrospinning and crosslinking of gelatin electrospun fibers loaded with microbial transglutaminase (mTG) enzyme. Firstly, the feasibility of electrospinning gelatin with mTG and the impact on electrospinning process and physical characteristic of the resulting fiber such as surface morphology and fiber diameter was investigated. Next, the efficacy of the crosslinking method was assessed. The stability of the fibers at physiological temperature and the post crosslinking structure were the two main characteristics examined. Different variables that may impact the crosslinking condition were also investigated to find the optimum crosslinking condition.

The second part of the project focuses on the use of bio- and cytocompatible synthetic material. Optimization of the coaxial electrospinning process is not elaborated in details as the concepts have been elucidated well in many other publications and it varies from one system to another. Method of incorporating chemotactic concentration gradient and the effect of imparting such gradient to the stability of the electrospinning process and the resulting fiber morphology were

established and analyzed. Subsequently, the existence of the encapsulated concentration gradient was showcased quantitatively and qualitatively. Lastly, the effect of NGF concentration gradient and the scaffold's cytocompatibility was demonstrated by directly seeding PC12 cells onto the electrospun fibers.

1.3 Report scope and outline

Chapter 1, the introduction, gives a concise account on the importance of tissue engineering, current adopted approaches and their limitations, and specification of the problem. Departing from this, the main idea that drives this project is elucidated. Specific objectives were laid out in the subsequent part. Lastly, scope and outline subsection briefly descriptively narrate the organization of this report.

Literature review in chapter 2 provides the basic and the reasoning of the general approaches taken in this project. Due to the interdisciplinary nature of tissue engineering and the enormous amount of information available, only more relevant concepts such as the relation between concentration gradient and neurite outgrowth, electrospinning, crosslinking of gelatin fibers and the use of mTG are elaborated more thoroughly.

Chapter 3 and 4 describe in detail the materials, experimental methods, results, discussion and conclusion of each sub-project aimed to fulfill first and second specific aim respectively. Next, in chapter 5, the results and their significance to the project in overall are briefly concluded. The potential application and direction of further research are proffered as well. Lastly, all the references are listed in Chapter 6.

2 Literature Review

2.1 Chemotaxis and haptotaxis in directing neurite outgrowth

Chemotaxis and haptotaxis are cellular behavior associated with directed motility or cellular projection in response to presence of graded distribution of diffusible and surface-bound extracellular bioactive molecules respectively. This graded distribution in concentration gradient format plays an important role in regulating cellular behavior and function. It has been well documented that the concentration gradient of bioactive molecules serves as guidance cues for cell migration, cell homing, morphogenesis, and neurite projection [1-8].

Nervous tissue is a prime example where concentration gradient is integral for development and function. In nervous tissue, the functionality is largely determined by the accurate specification of neurons and their target and the formation of orderly arrangement within the neuronal networks. It is therefore, in addition to mere growth and extension of neurites, direction to which the neurites are developed is another crucial factor, especially during the developmental and regeneration stage. Acting as guidance cues, these concentration gradients help the neurites to navigate to their target region and form contact with their appropriate postsynaptic partners. In case whereby nerve injury occurs, reestablishment of the connection in the same order prior to the injury is imperative to ensure functional recovery. These guidance cues can work either haptotactically or chemotactically, and work at either long or close range.

In vivo, such concentration gradient may be created by secretion of diffusible cues from distant source or by differential expression of non-diffusible cues bound to extracellular matrix (ECM). For a long neurite projection, a more complex guidance mechanism is required. In this case, the guidance is often assisted by intermittent short-range guidance cues positioned en route. The concentration gradient based regulation and guidance may involve a wide range of bioactive molecules. Neurotrophic factors, ECM associated molecules such as laminin, and some other protein families such as netrins, ephrins, semaphorins and slits, have been identified to be chemoattractant, encouraging neurites growth towards increasing concentration. Some other bioactive molecules, chondroitin sulfate proteoglycans (CSPGs), myelin associated glycoprotein (MAG), and Nogo-Am for examples, have antagonistic action, inhibiting the progression of neurite growth along their path [1, 3, 9-26]. In some cases, these bioactive molecules may also evoke bifunctional signals by being attractant to some type of neurons and repellent to others [18-22, 24-26]. Netrin, for example, promotes and guides the outgrowth of commissural [24] and retinal neurites [25] but proved to repel that of oligodendrocyte precursor cells in the embryonic spinal cord [26]. Varying in time and space, the orchestration of both attractive and repulsive cues guide the neurites along their designated path.

The extension and navigation of the neurites are helmed by a growth cone located at the tip of each neurites. Growth cone is a specialized amoeboid structure particularly sensitive to extracellular cues such as topography and concentration gradient of diffusible or surface-bound bioactive molecules. When exposed to concentration gradients, the extent of asymmetric occupancy of receptor for each particular guidance cues determines the decision to grow towards the concentration gradient or turn away from it. Several studies have shown that even shallow

extracellular concentration gradient can be converted into steeper gradient intercellularly or compartmentalized signals inside the growth cone through the generation of secondary messenger [27-29]. Disassembly and reconstruction of cytoskeleton at the growth cone soon follow in quick succession. In fact, the alteration in growth direction can be realized within minutes upon exposure to concentration gradient. In their study, Gundersen, R.W and Barret J.N subjected growing axons of chick dorsal root ganglion (DRG) neurons to diffusible NGF administered directly from a micropipette. The axons realized a positive turning response towards the NGF source within the course of 9-21 minutes [30]. Such a quick response is attributed to the capability of developing axons to locally translating protein in the growth cone [31-33]. This feature is indispensable as local translation enables the growth cone to promptly interpret guidance cues and responds correspondingly, especially to temporal chemotactic cues.

From in-vitro studies, the difference between the effect of concentration and concentration gradient has been clearly highlighted. The efficacy of the concentration gradient as guidance cue is more prominently determined by the gradient steepness rather than the concentration. In the analysis of diffusible NGF concentration gradient in their hydrogel setup, Cao, X., and Shoichet, Ms., found that gradient with a minimum of 133ng/ml/mm is required to effectively direct the neurite outgrowth from PC12 cells [34]. In their subsequent study this minimum concentration gradient threshold could actually be lowered to 80ng/ml/mm in the presence of equally steep gradient of neurotrophin-3 (NT-3) [12]. This study also indicates the possibility of enhancing the efficacy through synergistic effect of multiple concentration gradients.

2.2 Nerve growth factor

NGF belongs to the family of neurotrophin, a sub class of neurotrophic factors. Neurotrophic factors in general has a wide range of roles ranging from the contradictory action of promoting survival and selective cell death, maintaining cellular function to inducing differentiation and development of neuronal progenitor cells into neurons. Sharing a high degree of structural homology, neurotrophin family is comprised of NGF, NT-3, neurotrophin-4/5 (NT-4/5) and brain derived neurotrophic factor (BDNF). Nevertheless, these neurotrophins differs in their target specificity, membrane receptors, and distribution both spatially and temporally. Consequently, each of these neurotrophins may be preferentially more influential for different types of neurons and may play different role along the development path [35-37].

There are two receptors class for these neurotrophins, the low-affinity p75 neurotrophin receptor (p75NTR) and the high-affinity tyrosine kinase receptor (Trk). The tyrosine kinases receptors are consist of 3 subtypes, TrkA, TrkB, and TrkC. While all neurotrophins can bind to the p75NTR, NGF selectively binds only with TrkA, BDNF and NT-4/5 with TrkB, and NT-3 with TrkC. The action of Trks signaling is typically associated with survival and differentiation. On the other hand, the effect of the stimulation of p75NTR, depending on the context of the cells, may either promote survival or lead to apoptosis [38-40]. For instance, motor neurons (motoneurons) do not express TrkA receptors, hence their survival and function are regulated by other neurotrophins. The binding of NGF to p75NTR under the presence of nitric oxide would induce motoneuron apoptosis [39, 41, 42].

NGF is critical to maintain the survival and function of sympathetic and sensory neurons. In developmental stage, NGF is expressed and secreted by post-synaptic cells (target cells) to guide the neurite growth and promote maturation of pre-

synaptic cells. It has also been reported that in the case of injury, the expression of NGF and its associated receptor are upregulated in neurons and glial cells. Other than being neuroprotective, elevated expression of NGF at the distal end encourages directed neurites growth in the renervation effort [43]. While the level of NGF directly dictate the survivability of neurons, the NGF produced *in vivo* is in a minute quantities by the target cells and directly proportional to the innervation density [44].

PC12 cell, a cell line derived from rat sympathetic nervous system, is the standard in assessing the bioactivity of NGF *in vitro*. Greene, et al., found that PC12 cells, when cultured under serum-free condition underwent apoptosis upon withdrawal of NGF [45]. Furthermore, NGF also triggers the differentiation of PC12 cells, evidenced by the elongation and branching of neurites [45] and orients the neurite outgrowth towards positive concentration gradient [46-48]. This guidance effect elicited by concentration gradient of neurotrophic factors has been replicated in many *in vitro* studies, chemotactically [46, 49-53] as well as haptotactically [47, 54-56].

2.3 Integration of concentration gradient into engineered scaffold

The substantial role of concentration gradient has spurred many research efforts in attempt to integrate it into engineered scaffolds. The choice of method to generate the gradient, however, depends much on whether the concentration gradient is intended to invoke response haptotactically or chemotactically, the material used, and the route of which the scaffold is fabricated. A number of methods have been established to generate concentration gradient such as diffusion-based [12, 34, 57], pulsatile injection [46, 58], flow based [59-61], inkjet printing [62, 63], spatially

differential crosslinking [54, 56, 64] and adsorption [65]. Linear gradient maker is the simplest embodiment of flow-based method where two solutions with variable ratio are mixed and channeled out from single outlet.

To harbor the bioactive chemicals onto the surface, differential adsorption and immobilization are commonly adopted approaches [54, 56, 64, 65]. The bulk material can also be mixed with the bioactive chemicals and passed through a linear gradient maker prior to crosslinking process to create a graded distribution of immobilized molecules within the matrix [47]. Bioactive chemicals immobilized within PEG hydrogel microspheres with different buoyancies have also been used to create gradient scaffold [66]. The latter, however, presents a step-wise gradient rather than continuous gradient as can be obtained through the use of linear gradient maker.

Presenting concentration gradient of diffusible bioactive chemicals pose another challenge that the gradient needs to be maintained temporally to be within its therapeutic window. In comparison with immobilized concentration gradient, there are fewer methods apt for this purpose. Setups using microfluidic system can provide precise concentration gradient control, but this method is not easily scalable and integrated into any implantable scaffold [60, 61]. Moore et al., using a hydrogel sandwiched between two reservoirs with different concentration of NGF, have successfully created a stable and defined concentration gradient of NGF [12, 34]. However, without the continuous exposure to both reservoirs, the concentration gradient could diminish relatively quickly. Another method is to incorporate another delivery vehicle, such as microspheres, in the scaffolding material and adjust its spatial distribution within the bulk construct. Wang, X., et al. mixed silk microspheres encapsulating growth factors with alginate and using linear gradient maker to vary the

microspheres density prior crosslinking [67]. In such setup, the released amount and their gradient would be a direct function of microspheres density.

2.4 Electrospinning

2.4.1 Electrospun fibers as artificial scaffold

Natural ECM comprises of interconnected protein fibrils and fibers interwoven within a hydrated network of glycosaminoglycan chains. Fibers in similar scale mimicking ECM fibrillar component is particularly interesting as tissue construct. Compared to other fibers fabrication methods, the appeal of electrospinning owes to its simplicity and versatility in producing fibers in micro- and nanometer regime, which is in similar geometric scale with ECM fibrous components. In addition, due to their small scale and shape, electrospun fibers exhibit much larger specific surface area. Larger surface area allows more anchorage point for cell attachment and higher degree of surface functionalization such as modification in surface physiochemical properties, and bioactive molecules adsorption or immobilization.

Apart from their scale advantage, electrospun fibers have highly interconnected pores to mediate mass transport, possibility of tuning the mechanical properties, modification of their physiochemical properties, and easily biofunctionalized.

2.4.2 Process and underlying parameters

The electrospinning process itself is fairly simple. The basic setup requires only a pump to deliver the solution, a high voltage supply and a collector (Figure 3). Upon the application of sufficiently high voltage, the charged polymer droplets overcome the surface tension and assume a conical shape, from which a stream of

polymer jet then emerges. This cone is also known as Taylor cone. As the jet travels, the evaporation of solvent takes place causing the electrical charges to move to the surface. After covering short distance, this increasing repulsion forces in turn create instability and forcing the jet to experience a random whipping process. The polymer solution follows spiral trajectory along the electric field until the fibers are deposited on the collector. During the random whipping phase, the polymer solution elongates and solidifies [68-72].

A number of factors govern the electrospinning process and influence fiber diameter and morphology. These factors are categorized into factors that alter the solution properties and operating parameters. Concentration, polymer's molecular weight, type and mixture of solvents used, and inclusion of any other additives alter the conductivity and viscosity of the solution. The operating parameters cover the applied voltage, flow rate, tip to collector distance, and collector rotating speed. All of the above-mentioned factors need to be optimized in order to attain fibers with uniform size and morphology [72-74].

2.4.3 Selection of materials

The array of materials that can be electrospun is almost as extensive as the commonly available biomaterials and the list keeps on expanding, especially those of natural and synthetic polymers. The selection over which materials to use is subjected to the required mechanical properties and the surface physiochemical properties of the desired scaffold. Natural materials often have lower mechanical strength while typically offering superior cytocompatibilty and biocompatibiltiy compared to synthetic materials. In order to get the scaffolds with the right mechanical properties, cytocompatibiltiy, and biocompatibility features, it is a common approach to have a

blend of two or more materials. The blend may be among synthetic materials, natural materials, and combination of natural and synthetic materials. To address the mechanical properties and elasticity drawbacks, crosslinking process proves to be indispensable for natural materials. The degree of improvement, however, positively correlates to the degree of crosslinking. This controllable attribute creates the feasibility to fine tune the mechanical properties of the scaffold to match that of native tissue being replaced.

Materials of nature origin that has been widely used are gelatin [75-80], poly(saccharides) [79, 81-84], silk [85, 86], and materials derived from extracellular matrix such as collagen [87-91] and fibrinogen [92, 93]. While for synthetic material, the ubiquitous polymers are the most extensively used material due to their broad variety and versatility in modification. Among the most commonly used polymers are, poly(ester) family such as poly(lactic acid) [94-96], poly(glycolic acid [97, 98], poly(caprolactone) [99-104], poly(phosphoester) [105-107], and poly(ether) such as poly(ethylene glycol) [108, 109]) and poly(ethylene oxide) [110, 111]. Ceramics [112-117] and other strengthening component such as carbon nanotubes [117-120] have also been made as component.

2.4.4 Coaxial electrospinning

Coaxial electrospinning is a modified electrospinning process that uses two concentric spinnerets to simultaneously deliver two solutions to be spun concurrently (Figure 3b). As the result of such arrangement, the spun fibers exhibit distinct core-shell fiber structure. The main advantage of coaxial electrospinning compared to conventional uniaxial electrospinning is the feasibility of encapsulating non-electrospinnable materials. Nonetheless, the non-electrospinnable materials have to be

the core since it is still paramount for the shell materials to be electrospinnable in nature.

The optimization of coaxial electrospinning process is considerably more complicated compared to uniaxial electrospinning. In addition to all aforementioned factors, one has to further consider the difference of core and shell solution properties respectively and the ratio of both shell and core solutions flow rate. Several researchers have proposed the underlying process on how such core-shell fibers are created. It is hypothesized that the core solution is dragged by the shear stress generated at the interface of the solution [116, 121, 122]. Hence, naturally the shell polymer solution has to be more viscous than the core solution. The formation of double Taylor cone can be readily observed during stable electrospinning process.

Some researchers have suggested that in order to get distinct core-shell characteristic, it is a prerequisite for the shell and core solutions to be immiscible [116, 123]. However, some other studies have shown that in fact miscible solutions could also be used given that the viscosity of both shell and core solution are substantially different [121, 124]. The degree of mixing between the core and shell solution could become a chief concern as extensive mixing may imparts instability in the spinning process. The occurrence and the extent however are limited by the short contact period. The residence time of solutions in the Taylor cone is estimated to be in the order of 1s, while the characteristic time of random whipping phase is around 1 ms. As a comparison, the characteristic time of diffusion on a sharp boundary is significantly larger than that of random whipping phase but still smaller compared to residence time in the Taylor cone [121, 125]. This evidence suggests that the mixing, if there is any, occurs primarily in the Taylor cone.

In their application, coaxial fibers made from nature material shell and more rigid core material can avoid compromising the cytocompatibility while offering enhanced mechanical properties [126-128]. Moreover, coaxial electrospinning is increasingly pursued for creation of hollow fibers [113, 116, 122, 123], encapsulation of drugs [129-134], cells [135, 136], bacteria [137], and genes [104, 138, 139].

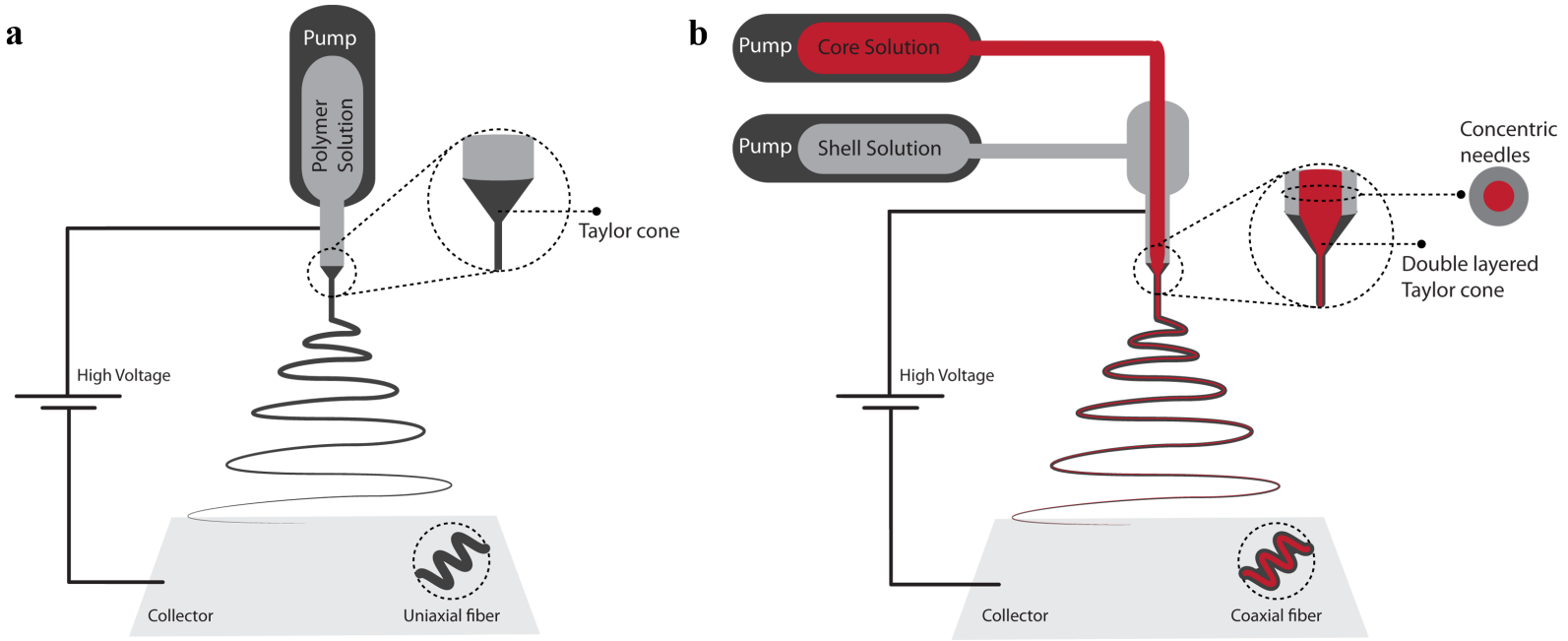

Figure 2.1. Schematic diagram of (a) uniaxial electrospinning and (b) coaxial electrospinning.

2.4.5 Bioactive molecules delivery from electrospun fibers

The versatility of electrospinning is not limited to only modification of fibers morphology or structure. The most interesting appeal of electrospinning may well be the ability to incorporate other additives such as bioactive molecules, carbon nanotubes, etc. As the result, delivery of bioactive molecules has been a ubiquitous functionalization of electrospun fibers. A wide variety of bioactive molecules has been successfully encapsulated and delivered, including proteins (for instance, growth factors [91, 105, 106, 131, 140, 141], and enzymes [142-145]), genes (for instance, viral gene [138], non-viral gene [104], DNA [139, 146], and short-interference RNA [147-149]), and drugs (for example, paclitaxel [150], ibuprofen [151], ketoprofen [152], doxorubin hydrochloride [153], vitamins [154] and antibiotics [155, 156]).

These bioactive molecules can be loaded before or after the fibers are created. Under the former category, bioactive molecules are usually added into polymer solution and then processed through uniaxial or coaxial electrospinning. Such incorporation can be easily done by blending the desired additives directly into the polymer solution [105, 106, 141-145, 147-160]. It is not necessary to have the additives dissolved in polymer solution as the additives may also come in suspended solid [161, 162] or emulsion [144, 145, 147, 153, 160, 163, 164]. While for post fibers production, these bioactive molecules can be loaded via absorption or harbored onto the surface through adsorption or crosslinking [64, 65, 118, 146, 165]. These different techniques are usually distinguished by their purpose. Functionalization via adsorption or crosslinking, for example, is more apt for application where the signaling is designed to come from surface bound bioactive molecules. On the other hand, absorption and direct incorporation in polymers solution are more geared toward delivery of diffusible bioactive molecules.

The release of bioactive molecules from electrospun fibers is generally found to be in sustained release manner. Sustained release of bioactive molecules from implant scaffolds has a great benefit for *in vivo* application. Not only the bioactive molecules are delivered locally, such long period availability also reduces the need to frequently change or administer the required bioactive molecules via other systemic or local route such as oral or injection. The rate of which bioactive molecules are released can be and need to be tailored and fine-tuned for each different bioactive molecule to be within the therapeutic level.

The release kinetic profile of bioactive molecules from electrospun fibers is highly dependent on the nature and interaction of the bioactive molecules and the polymer, and on which incorporation route pursued. When the drugs are directly added into the polymer solution and processed through uniaxial electrospinning, the bioactive molecules are typically uniformly distributed in the fibers. Another favorable approach is to have the bioactive molecules to be encapsulated inside the fibers via coaxial electrospinning. In this case, the bioactive molecules ideally are only located at the core of the fibers. This is particularly attractive for growth factors or other protein based drugs that are prone to degradation by exposure to harsh organic solvents often used in electrospinning. The only exposure would only be at the core shell interface during the electrospinning process.

Burst release of the encapsulated bioactive molecules is a prevalently observed phenomenon. It is due to the release of bioactive molecules that readily present on the surface upon contact with medium. While the core-shell format closely resembles reservoir-type of drug delivery system that characteristically has no burst release, many published studies have indeed reported such observation [104, 130, 132, 134]. This could possibly be caused by possible mixing or migration of the molecules to the

shell area during the spinning process. Compared to uniaxial electrospinning technique, the core-shell structure does suppress the extent of burst release [132].

Subsequent release of the remaining bioactive molecules requires the bioactive molecules to diffuse out from the fibers and regulated by the extent of the diffusion speed and the rate of which the fibers material degrade. When relatively fast degrading materials such as PLA or lightly crosslinked polymer were used, the release of the bioactive molecules can be primarily credited to bulk material degradation. However, when slow degrading materials are used, diffusion is the key driving force [166-168].

Controlling the release kinetic is another crucial factor in designing such bioactive molecules loaded scaffolds. For electrospun fibers, the use of co-polymers or blend of polymers, changing the extent of crosslinking to adjust the degradation rate and the use of porogens are widely adopted approaches to achieve such control [138, 140]. Porogens are usually easily water-soluble polymers or salts. Leached porogens create pores that help to accelerate the release of bioactive molecules from inside the fibers. Furthermore, the consequential porous structure speed up the degradation of the bulk material, thus allowing molecules entrapped within the polymer matrix to diffuse out.

In contrast to surface bound molecules where modulation of spatial distribution on fiber surface has been described [64, 65, 118, 165], thus far works with diffusible molecules have only been confined to their encapsulation, bioactivity upon release, and empirical evaluation of their release kinetic [105, 106, 141-145, 150-153, 155-160]. For the first time, we showed the possibility of introducing such spatial distribution to diffusible factors in electrospun fibers. The distribution of protein encapsulated in the core of coaxial fibers was tailored to be in concentration gradient format [169].

2.5 Use of electrospun fibers for neural tissue engineering

The use of electrospun scaffolds holds great promise in nerve tissue engineering, largely supported by the encouraging findings about neurons and glial cells behavior towards the fibrous architecture. Past research works has established that fibrous architecture provides the contact guidance cue for enhancement of neurite outgrowth, proliferation, differentiation and maturation [106, 170-181]. Variations such as cell type, alignment, fiber diameter, porosity, availability of bioactive chemicals such as growth factor and their spatial distribution and choice of material may affect the dynamics of neurite outgrowth and stem cell differentiation.

Fiber alignment has been found to be influential in promoting and guiding neurite outgrowth. When dorsal root ganglia (DRG) explant is cultured on random fibers, the neurites radiate from the explant forming a circular shape without any preferential direction. In contrast, on aligned fibers, the neurites emanate radially at the start but the projections parallel to the alignment grow faster thereby assuming elliptical shape [170, 171, 182, 183]. In one of the studies, compared to random fibers, highly aligned fibers increased the rate of outgrowth by 20% [171]. Other than DRG, similar observation has also been noted on embryonic hippocampal neurons [176], primary spinal motor neurons [184, 185], primary sensory neurons [185], PC12 cells [174, 186]. These neurons preferentially orient themselves with significantly longer neurite outgrowth along the fiber alignment.

Contact guidance cue provided by fiber alignment seems to exhibit the same effect on glial cells such as astrocytes and Schwann cells as well. Schwann cells migrated from DRG explant faster in the same direction as the fibers in tally with the extending neurites [171, 183]. In another piece of study, aligned fibers have been shown to enhance the maturation of Schwann cells [180]. On further note, with

astrocytes seeded on aligned fibers as feeding layer, the aligned morphology of the astrocytes helped to direct neurite outgrowth and cell migration from DRG explant [170]. These evidences show that the information of topographical cue can be communicated indirectly via cell-cell interaction. In addition, positive effects on Schwann cells are absolutely favorable for nerve regeneration as axon myelination is critical for signal transduction. Aligned fiber topography apparently benefits the differentiation of stem cells towards neuronal lineage too. Differentiating mesenchymal stem cells (MSCs) [178] and embryonic stem cells [187] on aligned fibers, compared to on random fibers, increased the expression of neuron-specific intermediate filaments.

Other than alignment, a few studies have also pointed out the effect of fiber diameter on the dynamic of cellular behavior. Being similar in scale with ECM fibrillar component and the cell itself, difference in fiber curvature may change the way cells perceive the surrounding. For instance, in Christopherson, et al. work, neuronal stem cells have 20% increased proportion towards neuronal lineage on 749nm fibers compared to 283nm and 1452nm fibers and 40% increase towards oligodendrocyte differentiation on 283nm fibers [179]. In another study, the neurite extension from DRG on 293nm fibers is 42% and 36% shorter than those on 759nm fibers and 1325nm fibers respectively [181]. However, the difference in diameter does not seem to have significant effect in Schwann cell migration [181].

Echoing the results of *in vitro* studies, *in vivo* implantation of electrospun fibers following nerve injury supports higher renervation and functional recovery [106, 183]. Kim et al., implanted both random and aligned poly(acrylonitrile-co-methylacrylate) (PAN-MA) to bridge peripheral nerve defect, without any incorporation of growth factors. The regeneration were significantly augmented by aligned fibers, but not with

random fibers [183]. In another piece of study, Chew et al. compared the performance of tubes made of plain aligned poly(ε ocaprolactone-co-ethyl ethylene phosphate (PCLEEP) fibers, aligned PCLEEP fibers with encapsulated BDNF, and smooth PCLEEP without any topographical cue for peripheral nerve regeneration. A number of indicative measures of successful regeneration such as axon myelination, nerve cross-sectional area, and ratio of axon diameter and myelinated fibers demonstrated the benefit of fibrous topography. While no functional recovery was noted for smooth tube, with only the plain fiber, 20% of the rats regained functional recovery. The chance of recovery was further bolstered to 44% when sustained release of GDNF was provided through encapsulation [106].

There are many influencing factors that takes part in restoring functional recovery. Although reported *in vivo* studies are still limited, these studies has elucidated the beneficial impact of fibrous topography, especially highly aligned fibers. Other than the inclusion of sustained delivery of drugs, other factors such as the effect of fiber diameter, and concentration gradient have not been tested out yet *in vivo*. Definitely, this warrant further close investigations as these factors may bring further improvement as it has been conclusively evidenced in *in vitro* studies.

2.6 Crosslinking of gelatin electrospun fibers

There are many established methods of crosslinking biopolymer but only a few have been successfully applied on electrospun fibers. The inabilities to preserve the fibrous morphology and interconnected pores have been specifically cited as the drawbacks. These methods can be commonly classified into two categories based on the need of having auxiliary agent usually termed as crosslinker. The first category is known as physical methods because it does not involve any crosslinker and relies on

physical treatment. On the other hand, the second methods, chemical method requires crosslinker.

Physical crosslinking can be achieved by dehydrothermal treatment (DHT), UV radiation, and use of plasma cleaner. DHT method employs low pressure (~0.05 bar) and high temperature (120-140^{o}C). The degree of crosslinking of gelatin fibers via DHT is reasonably high, estimated to be about 78% [188]. Although this method can be used to crosslink plain gelatin fibers, it becomes unfavorable when temperature sensitive drugs or protein is encapsulated prior crosslinking. UV radiation method, similar to other photo crosslinking, is hindered by limited penetration depth; therefore it is not suitable for crosslinking thick scaffold. The use of plasma cleaner generates reactive oxygen species for crosslinking. The resulting crosslinked fibers unfortunately are not thermostable as the fibers were reported to be completely dissolved within 12 hours at 37^{o}C[189].

Chemical method is a more commonly adopted approach to crosslink gelatin fibers. Vapor phase gluteraldehyde (GTA), glyceraldehyde, genipin, ethyl(dimethylaminopropyl) carbodiimide (EDC), ethyl(dimethylaminopropyl) carbodiimide-*N*-hydroxysuccinimide (EDC-NHS) have been successfully applied [75, 188, 190-195]. Adverse toxicity of residual crosslinker, byproducts and degradation product from hydrolytic or enzymatic degradation are usually chief concerns. GTA, for instance, although has been generally accepted to be an easy and effective way of crosslinking gelatin fiber, it is highly cytotoxic and may induce calcification of implant [196]. EDC facilitates interchain crosslinking within DNA. The dearrangement of DNA impedes cytokinesis and leads to cell death [197]. The use of glyceraldehyde and other α ehydroxycarbonyl compounds generates advanced gylation end products (AGEs) as the byproducts. AGEs has been identified to be cytotoxic and induce

oxidative stress and apoptosis on human promyelocytic HL-60 cells [198], rat primary cultured neurons [199], human mesangial cells [200] and retinal pericytes [201]. Repetitive soaking and rinsing are routinely done to reduce the amount of these toxic crosslinkers. Nevertheless, this process may incur significant lost of encapsulated materials.

Genipin has been advocated as a less cytotoxic alternative. However, the dissolubility of genipin in water imposes the use of organic solvent. Impregnating gelatin fibers in water/ethanol mixture containing genipin did not preserve the fibrous morphology, which is attributed to slower crosslinking reaction rate compared to the rate of hydrolysis [189, 192]. Removing the water entirely seems to help. Fibers soaked in genipin dissolved in ethanol for at least 3 days was reported to retain the fibrous shape [192]. Another method to improve the crosslinking is by incorporation of genipin during electrospinning. Choice of electrospinning solvents that could solubilize genipin appears to be greatly influential. It was reported that mix of gelatin and genipin spun out using TFE, the fibers underwent crosslinking *in situ* although substantial modification of morphology was observed [195]. In contrast, gelatin with genipin spun out from acetic acid requires further crosslinking in ethanol containing genipin for at least 3 days [192]. Furthermore, compared to glyceraldehyde and GTA, genipin has slower crosslinking kinetics [189].

2.7 Microbial transglutaminase and its applications in tissue engineering

Transglutaminases (TGs) are enzymes that catalyze covalent isopeptide bond formation between γ bcarboxamide group of glutamine and ndoup of glutami lysine residues by acyl transfer [202]. TGs mediated crosslinked products are usually highly resistant to thermal and proteolytic degradation due to the creation of inter- and intramolecular bond. Tissue transglutaminase (tTGs) present naturally in body fluids and tissue and take part in many activities, few among which are blood clotting, keratinization, stiffening of erythrocyte membrane, and stabilization of ECM [203-205]. In addition, intracellular tTGs has been shown to crosslink cellular protein during apoptosis [206]. An *in vitro* study recently has also suggested that tTGs plays role as regulator of chondrogenesis for mesenchymal stem cells [207].

The microbial counterpart, known as microbial transglutaminases (mTGs), is easier to produce and works well with substrate from both animal and plant origin [202, 208, 209]. Although both mTGs and tTGs perform similar function, there are few differences that set them apart. Compared to tTGs, mTGs are smaller in size (mTG mW~ 38k vs. tTG mw ~88k), has less substrate specificity, independent of Ca^{2+} and specific proteases to activate the enzyme [205, 210-212]. Many of these differences can be well explained by looking at the enzyme structure and amino acid sequence. The sequence of mTGs is very different from tTGs except for its sole Cys residue, which is crucial in catalyzing acyl transfer, and its surrounding physiochemical environment. Another notable difference is that mTGs lack the Ca^{2+} binding site common to tTGs. Characterization of tTGs has revealed a very low homology among them. However, their putative active Cys residue and Ca^{2+} binding domain are similar and exhibit highly conserved sequence [210]. In contrast with mTGs, the activity of

each particular tTGs is also regulated by the availability of their specific glutaminyl substrates. Fibrin/fibrinogen, fibronection, nidogen/ectatuin, osteonection, osteopontin, vitronectin, collagens are some that have been identified [205].

As naturally occurring enzymes, TGs have very low toxicity as elucidated in various studies. Bernard, B.K., et al. found that there was lack of signs of toxicity of mTG (2839 U/g active ingredient) administered to rat at a dose of 2000mg/ kg body weight. Moreover in the same study, the mutagenicity of mTG appears to be very low as well based on test on various strains of *Salmonella typhimurium* and chinese hamster lung cell line (CHL) [213]. In separate studies, addition of 0.05% of soluble mTG (specific activity: 27,000 nmol putrescine incorporated/mg/h) to fibroblast 3T3 cells culture showed cytotoxicity after 72 hrs. Concentration less than 0.05%, however, did not have significant effect compared to cells cultured on TCPS [214]. The difference in activity of mTG used in these studies may account for the discrepancy in reported results. The toxicity might be related to the activity mTG as well instead of only the amount. It is also unclear whether inactive mTG could elicit any toxicity as well. With further study, the toxicity effect can be further characterized.

The cytocompatibility of mTG crosslinked scaffolds have been verified by direct cell culture [214-220] and cells entrapment in hydrogels subjected to *in situ* crosslinking [221-224]. The entrapped cells proliferated well within the hydrogel, and maintained their sensing capabilities [221]. Kuwakara, K., et al. used gelatin-mTG injectable gel for *in vivo* cell delivery. The encapsulated cells were viable, proliferative and their release rate from the gel could be easily varied by regulating the amount of mTG. The use of mTG also allowed better integration of the gel with the surrounding tissue by forming bond between gelatin and endogenous collagen [224].

3 Microbial Transglutaminase Mediated Crosslinking of Gelatin Electrospun Fibers

Abstract

Crosslinking often becomes the major stumbling block in utilizing electrospun biopolymers, especially as sustained release vehicles. Issue of architectural integrity, crosslinking efficiency, toxicity, and harsh crosslinking condition effect on encapsulated bioactive molecules present multitude challenges. To address these concerns, we looked at feasibility and efficacy of using microbial transglutaminase (mTG) to crosslink gelatin electrospun fibers spun via acetic acid. The minimum concentration of gelatin with mTG to yield smooth fibers was found to be 25%. Microbial transglutaminase of up to 10wt% has negligible effect on spinning process and yield fiber with similar diameter (~400nm). Fiber size can be modulated instead by changing acetic acid concentration (~200nm, 400nm, and 550nm from 30, 40, and 50% acetic acid, respectively). The encapsulated mTG partially retained its catalytic function and the reaction occurred in the presence of moisture as provided by saturated water vapor. The degree of crosslinking, however, was limited and could not prevent dissolution at 37^{o}C Additional crosslinking by soaking in buffer solution containing mTG yield scaffolds with preserved fibrous architecture that lasts for up to 7 days at physiological temperature. Though the result was positive, but further refinement is needed to make it more suitable for imparting diffusible factors or their concentration gradient. Overall, we showcased that the mTG can be easily incorporated into electrospun gelatin fibers for crosslinking purpose.

3.1 Introduction

Foreign material may invoke hostile host response and toxicity issue, giving rise to sub-optimal performance and eventually implant failure. These negative reactions can be minimized through the use of bio-and cytocompatible materials and mimicry of ECM structure. Consequently, the interest in natural biomaterials for tissue engineering often stem from their superior bio- and cytocompatibility compared to their synthetic counterparts that can be easily capitalized on. In mimicking the ECM, electrospinning is a versatile and powerful method to produce fibers with similar scale to match native ECM fibrillar component.

Gelatin is natural biopolymer originated from partial hydrolysis of collagen. Despite being less ordered and lacking the signature triple helix structure of collagen, gelatin retains some of the functional amino acid sequences notably the integrin-binding domain [225-227]. In practice, gelatin alone is often used as scaffolding material or mixed with other polymers to enhance cytocompatibility or used as coating layer to promote cell attachment. The use of gelatin instead of collagen is compelling partly because of high tendency of collagen denaturation during scaffold fabrication. To electrospin collagen, the use of harsh organic solvent that leads to severe denaturation is unavoidable. The use of hexafluoroisopropanol (HFIP) and acetic acid, for example, only preserve about 12.5% and 29% of the characteristic triple helix structure [91]. This is clearly unfavorable, as only less than one third of the collagen remains. On the other hand, electrospun gelatin has been shown to have no change in structure [189].

Crosslinking process is paramount to improve gelatin's low mechanical strength and elasticity and lower its solubility in water. An additional requirement for scaffolds with defined architecture such as electrospun fibers is the preservation of the

structure detail. Among many established crosslinking methods, only a handful has been successfully applied to gelatin fibers. This includes physical methods such as dehydrothermal treatment (DHT) and UV radiation, and chemical methods such as the use of vapor phase gluteraldehyde (GTA), ethyl(dimethylaminopropyl) carbodiimide (EDC), ethyl(dimethylaminopropyl) carbodiimide-*N*-hydroxysuccinimide (EDC-NHS), glyceraldehyde, and genipin [75, 188, 190-195]. Physical methods are not suitable as the harsh crosslinking condition may denature preloaded bioactive molecules. On the other hand, toxicity of crosslinkers and their byproducts remains a serious issue [196-201]. GTA, for instance, has been reported to be highly toxic and may cause calcification of implant despite being quick and efficient [196]. Although genipin has much lower toxicity, it is much less efficient too compared to the use of GTA, EDC and glyceraldehyde [189, 192, 195].

An interesting and promising method that yet to be attempted to crosslink gelatin fibers is enzymatic crosslinking by transglutaminases. TGs are naturally occurring enzymes that catalyze formation of inter- and intramolecular isopeptide bond between glutamine and lysine residues [202]. In comparison with TGs produced by animal tissues, microbes derived TGs have several favorable features such as less substrate specificity, and lack of dependence on Ca^{2+} and specific ligand for activation [205, 210-212]. The use of microbial transglutaminase (mTG) is really attractive as it is biodegradable and has very low cytotoxicity [213-224]. Additionally, as typical to any other enzyme, the reaction that it catalyzes is site-specific thus leaving other functional groups to be unaffected. In this study, mTG was encapsulated directly inside gelatin fibers during electrospinning and the feasibility of using it to crosslink the fibers was assessed.

3.2 Materials and methods

3.2.1 Materials

Activa TG BW-MH microbial transglutaminase was obtained from Ajinomoto Singapore. The powdered product contain 1wt% microbial transglutaminase, ~99% maltodextrin, and a little amount of sodium chloride and sodium caseinate. Activa TG BW-MH reportedly contains 100 units of activity per gram-powdered preparation. Gelatin type B from bovine skin, hydrochloric acid (HCl), and sodium azide were purchased from Sigma Aldrich. Glacial acetic acid was purchased from Merck. PBS pH 7.4 (GIBCO) was bought from Invitrogen. Tris powder was obtained from Vivantis. The deionized water (DIW) has a resistance of 0.5 MΩ. All materials were used as received, without any further purification unless otherwise noted.

3.2.2 Electrospinning of gelatin-mTG

Acetic acid was used to prepare gelatin-mTG solution for electrospinning. In this study, there were 3 factors investigated, the concentration of gelatin, mTG loading amount, and the concentration of acetic acid used as solvent. The amount of mTG used is referred as percentage of powdered mTG with respect to gelatin weight. To prepare the solution, gelatin was first dissolved in more concentrated acetic acid and mTG was dissolved in DIW. Gelatin and mTG solution were mixed just before being electrospun and homogenous composition were ensured by rigorous vortexing for at least 15 minutes.

In order to find the gelatin concentration that could yield uniform fiber, 10-25wt% gelatin with 10wt% mTG in 5wt% step was dissolved in 40% acetic acid solution. The composition of gelatin and mTG is denoted as XG/YmTG with X and Y

being the concentration of gelatin and mTG respectively. The optimized operating parameters such as the flow rate, tip to collector distance, and applied voltage were determined in this step and used for subsequent studies. Rotating collector at low speed of around ~200-400 rpm were used to collect the fibers.

To investigate the impact of mTG loading amount, 3, 10, and 20wt% of mTG was incorporated into 25wt% gelatin in 40% acetic acid. The actual theoretical enzyme loading is 0.03, 0.1, 0.2 wt/wt% respectively Next, to determine the effect of varying the acetic acid concentration, 25wt% gelatin with 10wt% mTG were spun from 30%, 40%, and 50% acetic acid.

3.2.3 Crosslinking

The crosslinking was done via two steps procedure. At first, the fibers were exposed to saturated water vapor at room temperature in sterile condition. The period of exposure was set to range between 1-6 hours. In the subsequent step, the fibers were soaked in mTG containing buffer. 1wt% or 2wt% mTG was dissolved in 0.2M Tris-HCL pH 6 buffer. Prior to usage, the mTG solution was run through 0.2s as n was Tris-is-d in 0. The fibers were immersed for 1 and 4 hr for assessment. Afterwards, the scaffold was washed with PBS pH 7.4 three times for 10 minutes each to remove the remaining mTG for characterization.

3.2.4 Characterization

3.2.4.1 Fibers morphology

The as-spun fibers collected on aluminum foil were immediately transferred to vacuum oven and dried overnight. The fibers were sputter coated with platinum and

observed under scanning electron microscope (SEM). The fibers diameter was then measured by using open source software, Image J. A minimum of 70 fibers from each triplicate samples was measured for data analysis.

3.2.4.2 Crosslinked fiber morphology

Crosslinked fibers were first dehydrated via gradient ethanol, 30%, 50%, 70%, 90%, and 95% v/v (twice) for 15 minutes each. Next, the scaffold was dried by critical point drying method according to manufacturer protocol. Sputter coating with platinum was done immediately to minimize re-absorption of moisture. The following observation was performed under SEM. This study was done in triplicate.

3.2.4.3 Stability of crosslinked fibers

To evaluate the stability, the crosslinked scaffold was immersed at 37C in PBS pH 7.4 with 0.1wt% sodium azide as anti microbial agent. The scaffold structure was then analyzed after being incubated for 7 days. This study was done in triplicate.

3.2.4.4 Statistical data

Data is presented in the form of mean ± standard error of mean. The comparison between two groups was carried out using t-test. For comparison of 3 groups or more, ANOVA with post hoc analysis were done. Homogeneity of variance was tested prior determining the type of post hoc analysis. In comparing fiber diameter, games-howell post-hoc was adopted. 95% confidence level was used in all statistical analysis.

3.3 Results

3.3.1 Electrospinning

Gelatin dissolved in 40% acetic acid having concentration of 10-25wt% in 5wt% interval was spun together with the incorporation of 10wt% mTG. No stable electrospinning process could be obtained from 10G/10mTG and 15G/10mTG. Droplets instead of fibers were deposited on the target. Increasing the gelatin concentration to 20wt% (20G/10mTG) yielded fibers with beaded morphology. Smooth and uniform fibers could be spun with further increment of gelatin concentration to 25wt% (25G/10mTG). The optimized operating parameters were 10 cm for tip to collector distance, 0.8 ml/h for flow rate and -5/+13-15kV for applied voltage.

The effect of the incorporated mTG was determined by varying the mTG loading amount. Increasing the content of mTG from 3wt% to 10wt% did not seem to exhibit any significant effect, both to the electrospinning process itself and the resulting fiber morphology. The fiber diameter is not significantly different, 403.73±4.09 nm and 408.59±7.22 nm for 3wt% and 10wt% loading respectively. A loading amount of 20wt% however, was much more difficult to dissolve and there were solid remain even after vortexing. When tried being spun, the electrospinning process was not stable and the fibers obtained were wet and melded together at fiber-to-fiber junctions.

With variation of acetic acid concentration, while no notable difference was observed during the preparation of the spinning solution and the electrospinning process, the resulting fiber does show significant different in diameter. As tabulated in Table 3.1, the fiber diameter for 25G/10mTG fibers spun from 30%, 40%, and 50% are 210.65±5.35, 408.59±7.2, and 553.32±5.98 nm (ANOVA, $p<0.05$) respectively.

The surface morphology of these fibers was found to be smooth regardless of mTG loading amount and different concentration of acetic acid used for spinning. On further note, there was no difference in mTG solubility observed with different acetic acid concentration.

Samples	Mean (nm)	Std. Error (nm)
25G/3mTG-40% a.a	403.73	4.09
25G/10mTG-30% a.a	210.65	5.35
25G/10mTG-40% a.a	408.59	7.22
25G/10mTG-50% a.a	553.32	5.98

Table 3.1. As spun Gelatin-mTG fiber diameter

3.3.2 Crosslinking

As spun fibers which only exposed to water vapor dissolved in water as soon as it came into contact with water. Exposure to water vapor for at least 1 h renders the gelatin fibers insoluble at room temperature for up to 7 days, but completely dissolved at 37^{o}C within 3 hours. Extending the vapor exposure time up to 24 hours yielded the same outcome. The following impregnation in mTG solution helped to stabilize the fibers at physiological temperature.

Figures 3.2, 3.3, and 3.4 show the structure of the fibers subjected to different vapor exposure time and incubation in mTG solution time. When the fibers were exposed to water vapor for 1 h followed by incubation in 1wt% mTG for 2 h, the fibers experienced considerable structural deterioration. Nonetheless, when the water vapor

exposure was prolonged to 4 hours or longer, the structure can be retained. Incubation in 2wt% mTG for 2 h or in 1wt% mTG for 6 h or more proved to improve the morphology of 1 h water vapor exposed fiber. Nevertheless, no significant improvement was observed qualitatively by further increasing the incubation time or water vapor exposure period.

Inconsistency in crosslinking efficacy throughout the scaffold was also observed. In the same sample, as shown in Figure 3.5, transitional structures from fibers to film-like structure could be spotted.

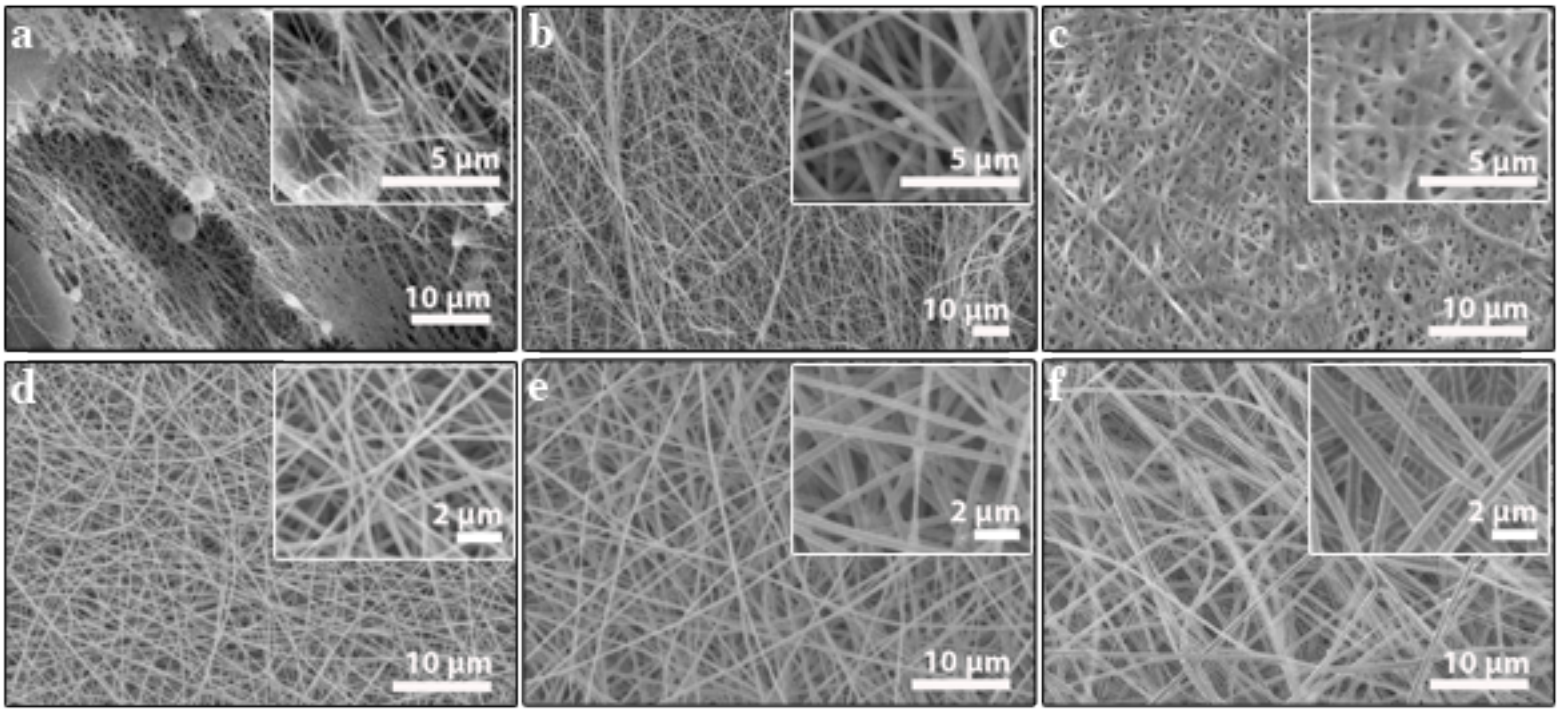

Figure 3.1a-f. As spun gelatin-mTG fibers via acetic acid (inserts are higher magnification images). (a) 20G/10mTG in 40% acetic acid. Beaded fibers were obtained. (b) 25G/3mTG in 40% acetic acid. (c) 25G/20mTG in 40% acetic acid, fibers were found merged together at the intersection. (d,e,f) 25G/10mTG in 30%, 40% and 50% acetic acid

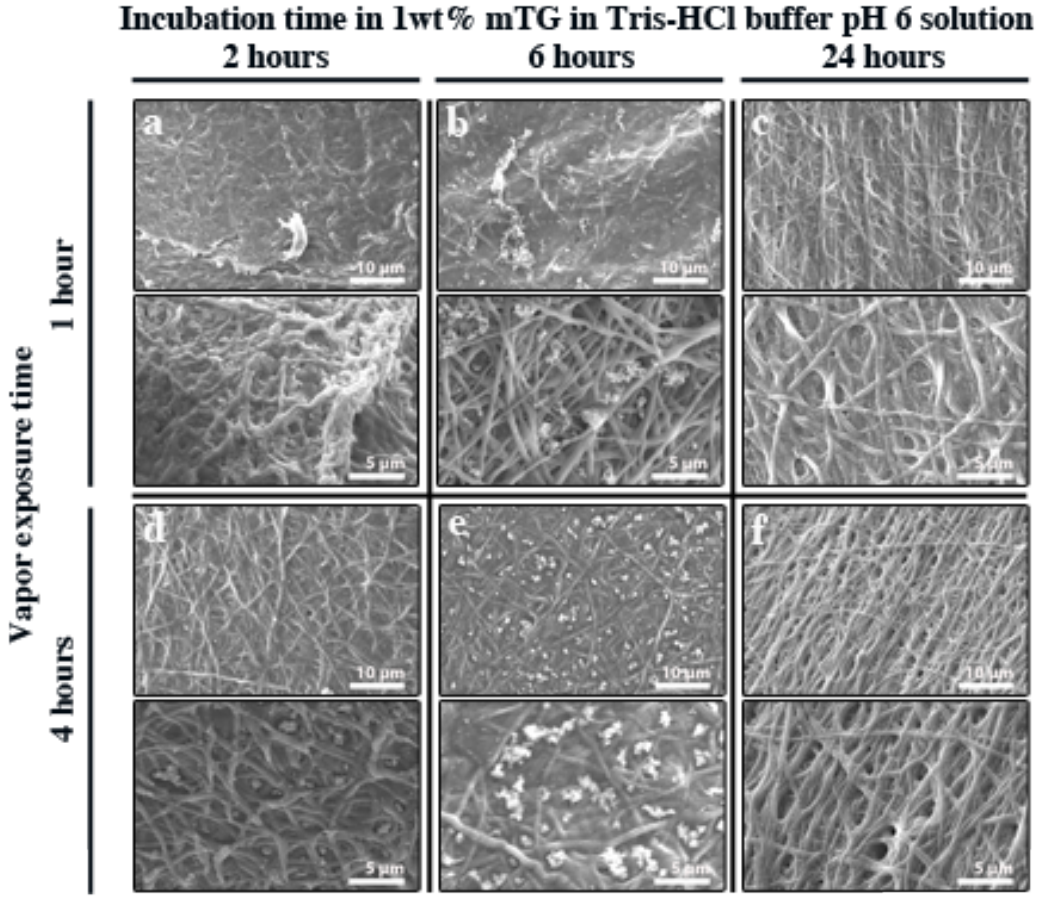

Figure 3.2a-f. Crosslinked fibers structure in 1wt% mTG in Tris-HCL buffer pH 6 solution. (a-c) fibers were exposed to water vapor for 1 hr and soaked for 2, 6 ,and 24 h respectively. (d-e) fibers were exposed to water vapor for 4 h and soaked for 2, 6 ,and 24 h respectively. Fibrous shape was maintained in all crosslinking condition, with the exception in (a) where the fibers showed sign of deterioration.

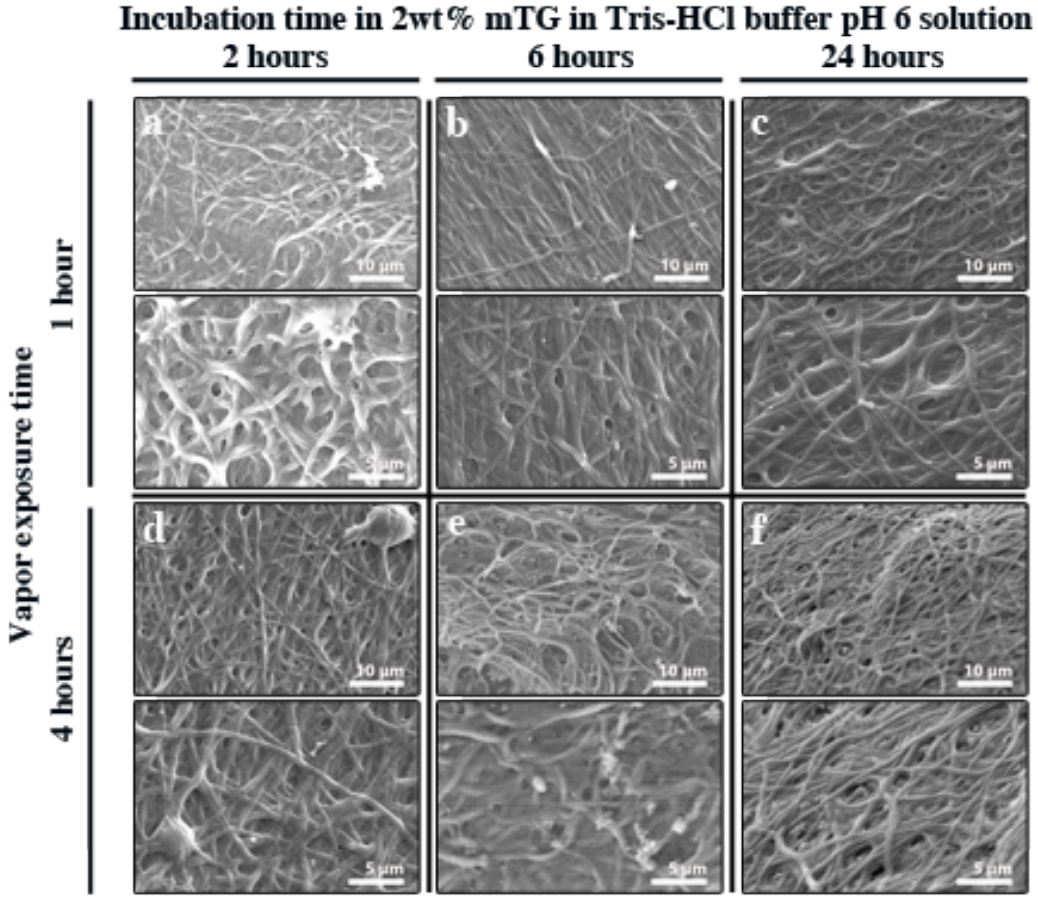

Figure 3.3a-f. Crosslinked fibers structure in 2wt% mTG in Tris-HCL buffer pH 6 solution. (a-c) fibers were exposed to water vapor for 1 h and soaked for 2, 6 ,and 24 h respectively. (d-e) fibers were exposed to water vapor for 4 h and soaked for 2, 6 ,and 24 h respectively. Fibrous shape was maintained in all crosslinking condition.

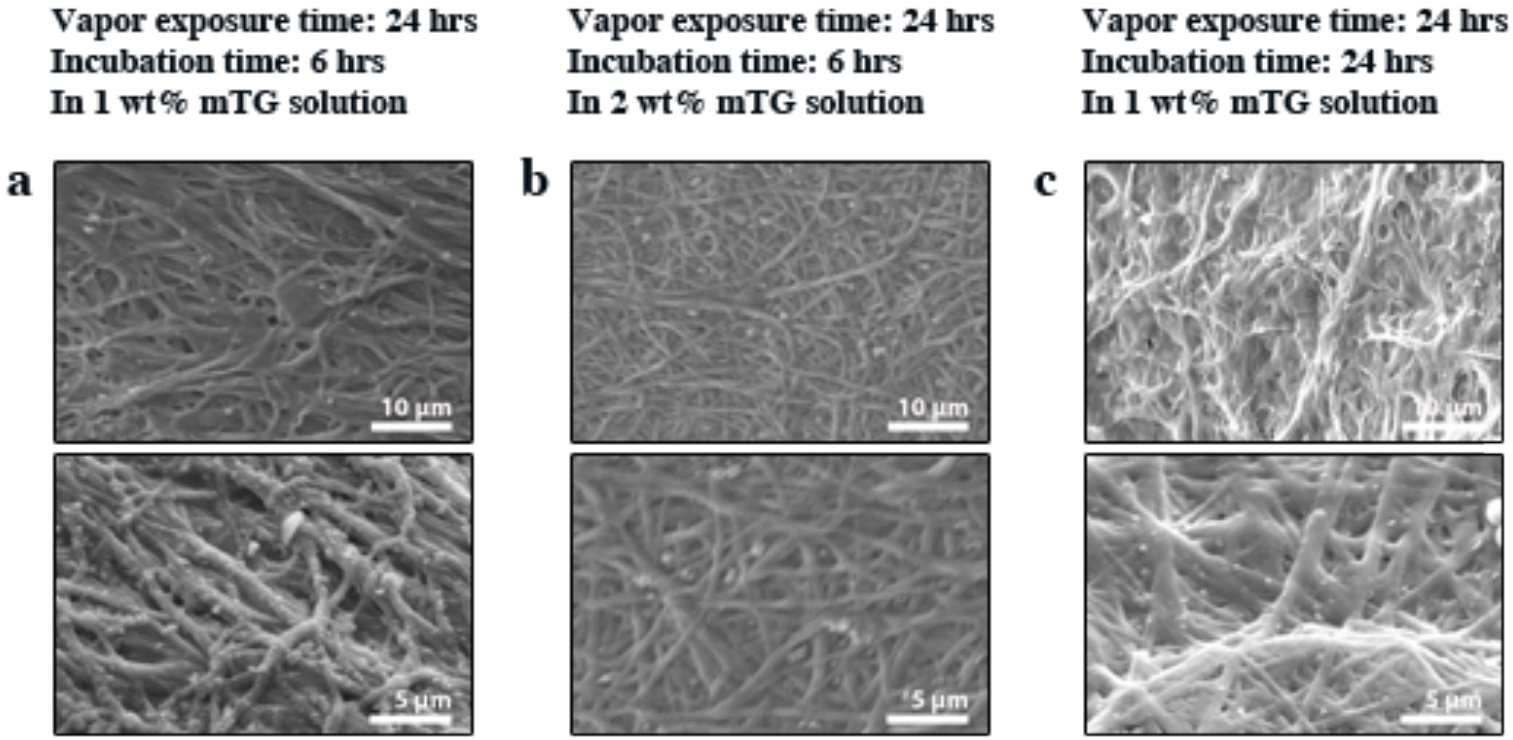

Figure 3.4. Crosslinked fibers structure of 24 h water vapor exposed fibers followed by incubation in mTG solution. (a&b) incubation in 1 and 2wt% mTG solution for 6 h, and (c) incubation in 1 wt% mTG solution for 24 h. Compared to shorter water vapor exposure time, there is no significant structural improvement achieved.

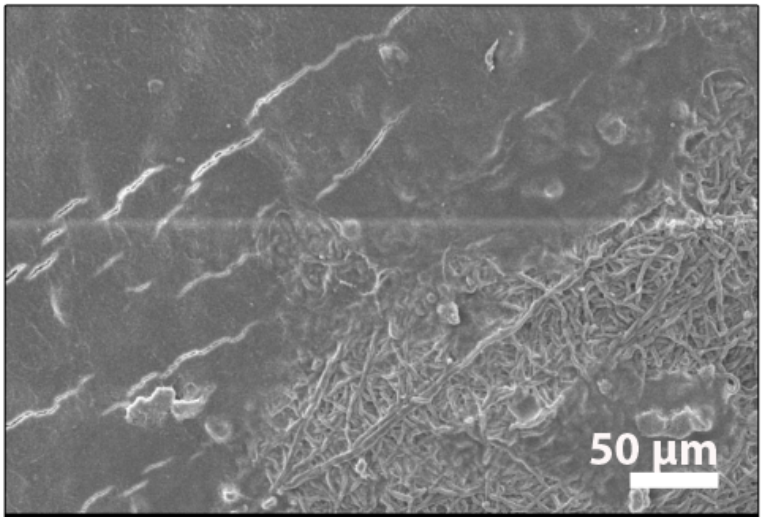

Figure 3.5. Fiber-film transitional structure. Fibers lost their individual structure and merged together to form film.

3.4 Discussion

Concentration of the polymer is one of the crucial factors in electrospinning. Depending on the type and mixture of solvents, the critical concentration to yield smooth and uniform fibers may differ. Using 40% aqueous acetic acid as the solvent, it was found that a minimum of 25wt% of gelatin is needed to obtain uniform fibers. In line with typical observation of electrospinning process, too low concentration translates to spraying of droplets. This is caused by insufficient viscoelasticity to withstand the surface tension force. The transition from droplets to beaded fibers (Figure 3.1a) and eventually to smooth fibers is in tandem with increasing concentration and viscoelasticity of gelatin solution.

The addition of mTG from 3-10wt% did not show any significant difference in electrospinning process and the resulting fiber diameter. Doubling the content to 20wt% however, posed instability to the spinning process. Optimization of other

parameters such as flow rate, applied voltage and distance did not improve the quality of the fibers obtained. As shown in Figure 3.1c, the fibers merged together at the fiber-fiber intersection and covered most of the pores. In addition the presence of solid matters despite vigorous vortexing was evident. Such high amount of mTG may well exceed its solubility limit in gelatin solution. Concentration of acetic acid was found to be more influential to fiber diameter. Holding the gelatin and mTG amount constant, the fiber diameter increases as the concentration of acetic acid increases. Similar observation has also been reported. With porcine skin gelatin concentration held constant at 10%, the fiber diameter increases from 103nm to 148nm when acetic acid concentration was increased from 80% to 90% [80]. The difference in minimum concentration and acetic acid strength in the reported study may stem from the different source and molecular weight of gelatin used.

The crosslinking efficacy was assessed through the stability of the scaffold at physiological temperature for prolonged period and morphology of the crosslinked scaffold. The as-spun fibers readily dissolved upon contact with water at room temperature despite incorporation of mTG. Furthermore, the solution viscosity remained unchanged when the homogenous gelatin-mTG solution was let to stand at room temperature for 7 days and the fibers spun from the solution yield the same morphology as that of freshly prepared solution. All together, this suggests that no crosslinking reaction occurred since the mTG was introduced to gelatin solution and during the electrospinning process. This could be attributed to inconducive condition caused by the low pH of the solution. The working pH range of mTG is reported to be from 4 to 9 [228]. For comparison, 30% acetic acid, the lowest concentration acetic acid solution used in this study, has a pH value of 2.03.

Exposure to water vapor provides moisture that facilitates crosslinking reaction *in situ*. This was obvious since fibers kept well in desiccator for extended period up to 14 days still immediately dissolved in water upon contact. Water vapor mediated step is critical as any facilitating crosslinking method involving direct immersion in mTG containing buffer solution, is not feasible. This is because the dissolution rate of gelatin fibers in water is faster than the crosslinking rate. Impregnation in gelatin non-solvent, such as ethanol, is not desirable as well as it may deactivate mTG. Cui, L., et al., reported that although the activity of mTG can be slightly increased in the presence of 10% ethanol, at higher concentration the catalytic capability deteriorates rapidly [229].

Nevertheless, simply providing moisture through water vapor exposure was not enough to grant thermal stability at physiological temperature. At this stage, low pH would not be the major inhibiting factor anymore as almost all of the solvent would have evaporated by the time the fibers were deposited during electrospinning process. It is more likely that such limited crosslinking process was caused by inadequate amount of active mTG. The activity of any enzyme depends on the preservation of its functional 3D structure. Low pH and high voltage may cause change to mTG structure conformation. Moreover, the use of impure mTG and low enzyme activity contributed to inefficient crosslinking.

In order to increase the fibers stability at physiological temperature, further crosslinking process is then compulsory. Following water vapor exposure, the fibers were soaked in mTG solution in tris-HCL buffer. The pH was adjusted to 6 as it was reported that mTG activity is enhanced at this condition [230]. The concentration of mTG in the buffer, however, was limited by mTG powder solubility. Above 2wt%, the powder tends to agglomerate. The results suggest that there is a trade off between the

crosslinking rate, incubation time and crosslinking extent during water vapor exposure. The lack of crosslinking during water vapor exposure can be offset by either increasing soluble mTG concentration or incubation time (Figure 3.2, 3.3 and 3.4).

Albeit achieving major structural improvement, a major setback was encountered in this study. Fibers-film transitional structure was randomly found on the samples (Figure 3.5). We hypothesized that it is due to non-uniform crosslinking across the scaffold during water vapor exposure period. The swelling of these fibers in aqueous medium highly depends on how tight the gelatin molecules are crosslinked. Loosely crosslinked fibers during the first step may cause excessive swelling and prone to merge together with adjacent fibers during the incubation step. Therefore, the key step in preserving the fibrous architecture is the crosslinking that occurred during exposure to water vapor. The crosslinking extent should exceed the certain threshold to ensure the structural integrity of individual fiber. Crosslinking rate and extent depend not only the amount but also on the enzyme activity level. The use of higher activity mTG with fewer impurities may improve the crosslinking efficiency. It is also possible that use of more active mTG would not require any additional crosslinking.

The fact that the latter part of crosslinking method necessitates incubation in aqueous medium presents disadvantages when diffusible factors are encapsulated during electrospinning. A huge percentage of the drugs may diffuse out of the fibers as, compared to synthetic materials, the hydrogel nature of gelatin fibers supports higher diffusion rate.

3.5 Conclusion

We have demonstrated that mTG can be easily incorporated into gelatin fibers and partially retained its catalytic function. However, the fibers did not undergo crosslinking during the electrospinning process. The crosslinking has to be done via two steps procedure, provision of moisture via water vapor exposure and further crosslinking in mTG solution, to make the fibers thermally stable at physiological condition and retain their fibrous structure. Nonetheless, the supplemental immersion and suboptimal crosslinking are two great concerns. With the current state of the result, it is still unsuitable to confer any diffusible bioactive chemicals or their concentration gradient. Further and more comprehensive studies need to be carried out to improve the crosslinking process and better characterize the scaffold in terms of their post-crosslinking structure, drugs retention capability, and cytocompatibility. Given its low toxicity and biodegradable nature, mTG crosslinked fibers may appeal to broad spectrum of applications in tissue engineering.

4 Nanofibrous Scaffold with Incorporated Protein Gradient For Directing neurite outgrowth[1]

Abstract

Concentration gradient of diffusible bioactive chemicals assumes many important roles in regulating cellular behavior. Amongst many factors influencing functional recovery after nerve injury, such as topographical and biochemical signals, concentration gradients of neurotrophic factors provide chemotactic cues for neurite outgrowth and targeted renervation. In this study, a concentration gradient of nerve growth factor (NGF, 0-250 μg/ml) was incorporated throughout the thickness of poly(e-caprolactone)-poly(ethylene glycol) coaxial electrospun nanofibrous scaffolds (~ 700 μm thick with ~ 800 nm average fiber diameter). The existence of the protein gradient upon protein release was demonstrated using a customized underagarose-PC12 neurite outgrowth assay. When exposed to scaffolds endowed with NGF concentration gradient (NGF-CG), significant difference in the percentage of cells bearing neurite outgrowth was observed (7.1 ± 1.9% vs. 0.8 ± 0.3% for cells exposed to high vs. low concentration surface respectively, $p < 0.05$). In contrast, no significant difference was observed when cells were exposed to scaffolds that encapsulated a fixed concentration of NGF. Direct culture of PC12 cells on the substrates

[1] This chapter has been published in whole. Changes made to figures and references numbering are to conform to the style and flow of this thesis.

Handarmin, G J Y Tan, S Bibekananda, G T Marcy, E L K Goh and S Y Chew, *Nanofibrous scaffold with incorporated protein gradient for directing neurite outgrowth*, Drug Delivery and Translational Research, 1(2), pp. 147-160, 2011, doi: 10.1007/s13346-011-0017-3.

demonstrated the cytocompatibilty and the effect of diffusible NGF gradient on neurite outgrowth. A significant difference in the percentage of cells with neurite extensions was observed when PC12 cells were seeded on NGF-CG scaffolds (21.2 ± 3.6 % vs. 10.4 ± 1.3 % on high vs low concentration surface respectively, $p < 0.05$). Furthermore, Z-stack confocal microscopy tracking of neurite extensions revealed the chemotactic guidance effect of NGF concentration gradient. Directed and enhanced neurite penetration into the scaffolds, towards increasing NGF concentration were observed. *In vitro* release study indicated that the encapsulated NGF was released in a sustained manner for at least 30 days (80.4 ± 3.6 % released). Taken together, this study demonstrates the feasibility of incorporating concentration gradient of diffusible bioactive chemicals in nanofibrous scaffolds via the coaxial electrospinning technique.

4.1 Introduction

Concentration gradients of diffusible biochemicals provide chemotactic cues to direct biological responses such as cell migration, tissue morphogenesis, and neurite outgrowth [231-233]. In nerve regeneration, targeted renervation is crucial for promoting functional recovery and the direction of neurite extension may be regulated by physical and biochemical signals such as topography and the coordination of stimulative, inhibitive and directive biomolecules [234, 235].

In vitro, the mere presence of neurotrophic factors promotes neurite outgrowth from neuronal cells such as PC12 cells and dorsal root neurons. Presented in a concentration gradient format, neurotrophic factors preferentially guide neurite projections in the direction of the positive gradient. [34, 49, 50, 55, 236-238]. While the benefits of incorporating concentration gradients for directing cell fate are clear, translating these *in vitro* works into *in vivo* implementation remains a challenge. One of the obstacles is the difficulty in integrating the technique of generating concentration gradients into scaffold fabrication methods. Microfluidic devices, for instance, can produce controllable and very precise concentration gradients of biochemicals [239-241]. However, such methods cannot be scaled up easily and may not be used directly to create scaffolds in a simplistic manner for direct implantation. In addition, most studies have focused on hydrogels [34, 57, 242-244]. While these isotropic materials are useful platforms for direct *in vivo* implantation, it is often difficult to incorporate topographical cues for a synergistic effect to direct cellular behavior.

Structurally, electrospun scaffolds closely mimic the native extracellular matrix (ECM), comprising of sub-micron to nano-sized fibers that are similar in geometric scale as ECM fibrillar components. Such biomimicking substrates may provide

physical cues to direct cell fate [179, 180, 245, 246] and enhance nerve regeneration [106, 181, 247]. The versatility of the electrospining process has also allowed the implementation of these nanofibers as surface coatings to enhance neural electrode implant-tissue integration [248-250].

In tissue regeneration, the sustained availability of biochemicals is often necessary over an extended time period. Since these diffusible bioactive chemicals and their concentration gradients are often subjected to changes by interstitial fluid flow and biodegradation, a good controlled release vehicle is required. Drug-encapsulated electrospun fibers can serve as ideal drug delivery vehicles with sustained release behavior [105, 106, 129, 133, 140, 251, 252]. In particular, coaxial electrospun fibers provide greater protection over the encapsulated biomolecules than conventional uniaxial fibers. This is due in part to the physical separation of the drugs from organic solvents that are typically used during electrospinning. Moreover, drug release rate can be fine tuned easily in coaxial electrospun nanofibers [129, 133, 138, 140, 141, 253].

In this study, we incorporated a concentration gradient of nerve growth factor (NGF) into nanofibrous scaffolds via coaxial electrospinning. We demonstrate the feasibility of fabricating a biomimicking scaffold that is endowed with a combination of nanofiber topography, sustained availability of NGF and a concentration gradient of the encapsulated protein. Such biofunctional substrates may find useful applications in directing neurite outgrowth for enhanced nerve regeneration and neural electrode implant-tissue integration.

4.2 Materials and Methods

4.2.1 Materials

Poly (e-caprolactone) (PCL, Mn 80,000), poly(ethylene glycol) (PEG_{3350}, Mw 3350 and $PEG_{35k,}$ Mw 35,000), bovine serum albumin (BSA) with fraction V ≥ 96%, fluorescein isothiocyanate-bovine serum albumin conjugate (FITC-BSA), sodium azide, dichloromethane (DCM), 2,2,2-trifluoroethanol (TFE) with purity 99.0%, Tween 20, 45% D-(+)-glucose solution, 10% formalin, Triton-X, and glycine were purchased from Sigma Aldrich, USA. RPMI 1640 with L-Glutamine, heat inactivated horse serum, fetal bovine serum (FBS), and HEPES free acid 1M solution were purchased from Hyclone. Phosphate buffered saline (PBS), pH 7.4, antibiotic and antimycotic, sodium pyruvate 100 mM 100X (GIBCO), phalloidin - Alexa fluor 633, phalloidin - Oregon green, DAPI, and Live/Dead Vialibility/Cytotoxicity Kit for mammalian cells (Molecular Probes) were purchased from Invitrogen. The deionized water has a resistance of 0.5 Mar Probes) were purchased from Invitrogen. nvitroand recombinant human β nNGF duo set ELISA kit were purchased from R&D Systems. NGF was reconstituted in sterile 0.1 wt% BSA solution. Pierce BCA protein assay was purchased from Thermo Scientific. Mouse collagen type IV was from BD-Biosciences and agarose was purchased from Bio-Rad. Tissue Tek O.C.T compound was obtained from Fisher Scientific. All materials were used as received without any further purification unless otherwise noted. PC12 culture medium comprised of serum free RPMI supplemented with 1% sodium pyruvate, 1% HEPES, 1% antibiotic-antimycotic solution and 0.267% glucose.

4.2.2 Scaffold fabrication

Coaxial electrospun fibers were prepared using a custom-made coaxial setup. The core solution was fed through a 22G needle configured concentrically within a 1.5 mm wide circular opening on the coaxial chamber. For all samples, the composition of the shell solution was fixed and comprised of 10 wt% PCL in TFE with 20 wt% PEG_{3350} (with respect to PCL) as the porogen. A fixed concentration of core solution diluent was also used for all samples. This core diluent comprised of 150 mg/ml of PEG_{35k}.

The protein concentration gradient within the core of the nanofibers was generated using a linear gradient maker that was connected to a peristaltic pump (CBS Scientific Co.), as shown in Figure 1. The gradient maker consisted of two equivolume chambers, A and B, that was connected by a 200 ml conduit. A Teflon valve was inserted at the center of the conduit to control fluid flow between the two chambers. To fabricate scaffolds comprising of a gradient of carrier protein, BSA, only (denoted as BSA-CG, where CG indicates concentration gradient, Table 1), 600 ml of concentrated BSA solution (40 mg/ml reconstituted in core diluent) was loaded into chamber A, while chamber B comprised of 900 ml of core diluent. A magnetic stirrer was placed in chamber B to ensure thorough mixing of the solutions. To fabricate scaffolds comprising of NGF concentration gradient (denoted as NGF-CG, Table 1), an additional 150 mg of NGF was added into the concentrated BSA solution in chamber A. The theoretical loading levels of NGF and BSA were 0.04% and 10.58% respectively with respect to the dry weight of the scaffolds. BSA was used as a carrier protein to protect and stabilize NGF. The theoretical NGF concentration gradient encapsulated throughout the thickness (~ 700 μm) of the scaffold was 0-250 μg NGF/ml of core solution.

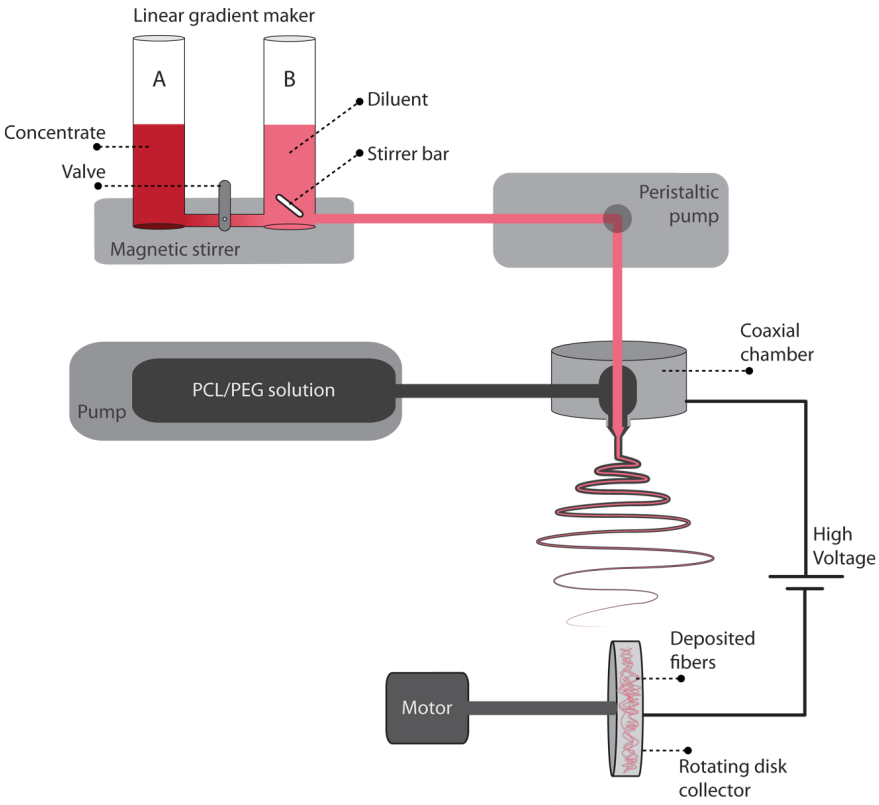

Figure 4.1. Schematic diagram of coaxial electrospinning setup.

Preliminary experiments conducted to determine the efficiency of the linear gradient maker showed that only ~ 65% of BSA in chamber A was dispensed out over a 2 h period. Based on this efficiency, the amount of protein required to fabricate scaffolds with fixed protein concentrations was adjusted proportionally so that the theoretical loading levels of BSA and NGF remained the same as scaffolds with protein gradients. To fabricate scaffolds with fixed concentration of BSA (denoted as BSA-FC, where FC indicates fixed concentration, Table 1), 25 mg of BSA was reconstituted in 1 ml of core diluent. For scaffolds with fixed NGF concentration (denoted as NGF-FC, Table 1), 100 µg NGF was added along with 25 mg of BSA into

1 ml of core diluent. The respective core solution was then loaded into the coaxial chamber by a syringe pump (New Era Pump System) for electrospinning. The compositions of the electrospinning solutions used in this study are summarized in Table 1.

All samples were collected on a negatively charged rotating mandrel that was 12 cm in diameter (total deposition area = 75.4 cm^2). The rotation speed of the collector was set at ~400 rpm and the tip-to-collector distance was 14-15 cm. A voltage of - 4/ +17-22 KV was applied for electrospinning. The flow rates of the core and shell solutions were set at a ratio of 4:1, with 4 ml of the shell solution delivered at a rate of 2 ml/h. The electrospinning process was carried out for 2 h, resulting in a scaffold thickness of ~700 μm.

Shell Solution Composition	Core Solultion Composition			Encapsulation format	Notation
	PEG_{35K}	BSA ~25mg/ml	NGF ~100g/mll		
10wt% PCL + 20wt% PEG_{3350}	150mg/ml	+	-	Concentration gradient	BSA-CG
		+	-	Fixed concentration	BSA-FC
		+	+	Concentration gradient	NGF-CG
		+	+	Fixed concentration	NGF-FC

Table 4.1. List of experimental samples and notation used.

4.2.3 Characterization

4.2.3.1 Fiber morphology and core-shell structure evaluation

As-spun fibers were dried under vacuum overnight and sputter coated with platinum (JEOL JFC-1600) prior to observation by the scanning electron microscope (SEM) (JEOL JSM-5500). Fiber diameters were measured using the open-source image processing software, ImageJ. At least 100 fibers were measured for each sample group. To examine the core-shell structures of the nanofibers, the scaffolds were rolled into tubular form and cut perpendicularly in liquid nitrogen using a surgical blade. The revealed cross section was then dried, sputter coated and analyzed under the SEM.

4.2.3.2 Protein gradient visualization

0.05 wt% of FITC-BSA was added into the BSA solution during the fabrication of BSA-CG scaffolds, to create a gradient of FITC-BSA throughout the scaffold. Thereafter, the scaffold was embedded in O.C.T. and sectioned at a thickness of 50 μm using a cryostat (Leica CM1900) prior to observation under an epi-fluorescent microscope (Olympus, DP71).

4.2.3.3 Quantification of protein gradient

In order to quantify the concentration of protein encapsulated within the fibers, BSA-CG fibers (average weight 33 ± 2 mg) were collected for a 5 min duration at fixed time points. Thereafter, the fibers were dissolved in 1 ml of DCM. One ml of PBS was then added and the mixture was vortexed and equilibrated at room temperature for 15 min. Following that, the mixture was centrifuged at 4000 rpm for 5 min and the aqueous medium was retrieved. Another 1 ml of fresh PBS was added and

the entire process was repeated. For comparison, the core solution of BSA-CG scaffold was collected for the same duration at the same time points directly after dispense from the linear gradient (prior to electrospinning). Finally, the concentration of BSA was determined using Pierce BCA assay. Both experiments were conducted in triplicates.

4.2.3.4 Release kinetics

The release kinetics studies were conducted under dynamic conditions at 37^{o}C, 50 rpm (Heidolph Polymax 1040). NGF-CG (average weight = 134 ± 10 mg, n = 3) and BSA-FC (average weight = 255 ± 5 mg, n = 3) scaffolds were incubated in 5 and 7 ml of PBS with 0.01 wt% of sodium azide respectively. At predetermined time points, 2 ml of supernatant was retrieved and replaced with an equal volume of fresh PBS. After each release profile reached a plateau, all remaining proteins were extracted from the scaffolds following previous protocol for quantifying BSA protein gradient. Finally, the concentrations of NGF and BSA were determined using ELISA and Pierce BCA assays respectively. The experimental protein loading efficiencies were computed using the following equation:

$$Loading\ efficiency = \frac{(cumulative\ amount\ of\ protein\ released + extracted\ protein)}{original\ protein\ loading} x100\%$$

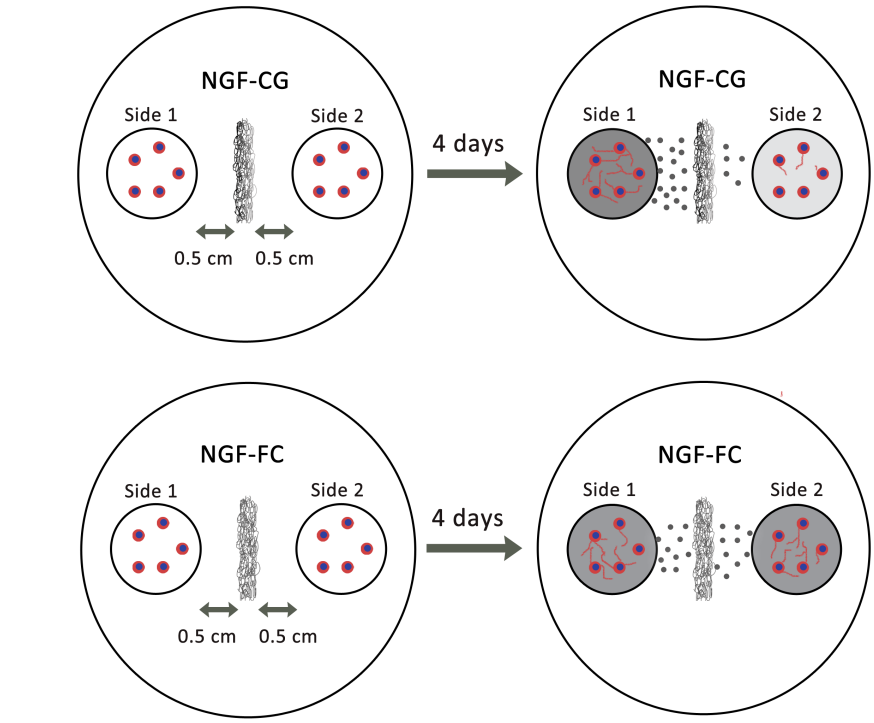

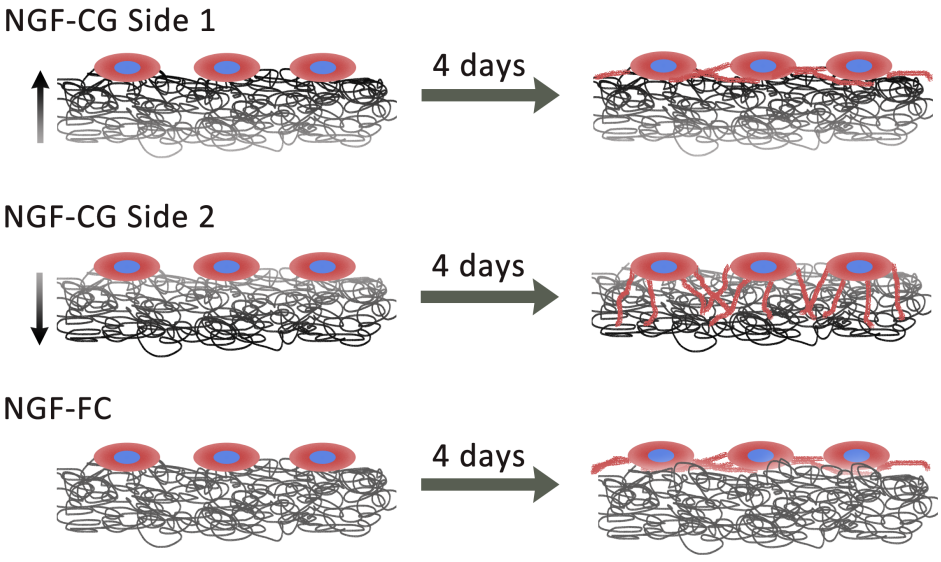

Figure 4.2. Schematic diagrams of (a) customized underagarose assay and (b) PC12 direct culture experiment using NGF-CG and NGF-FC scaffolds. Grayscale intensity gradient represents NGF concentration gradient. Arrow: direction of increasing NGF concentration.

4.2.3.5 Underagarose assay

A customized underagarose assay was designed to test the efficacy of the scaffolds in directing the extent of neurite outgrowth. Twenty ml of 1 wt% agarose in serum free RPMI (0.22 mm filtered) was casted into a customized mold within a 6-cm petri dish to result in the configuration shown in Figure 2a. Prior to cell culture, a glass coverslip was placed within each well at an equidistance of 0.5 cm from the center rectangular cavity. Five ug/cm^2 of collagen IV was then added to coat the coverslips for 1 h at room temperature. Thereafter, the coverslips were washed with sterile PBS twice and the wells were equilibrated in serum free RPMI at 37^{o}C, 5% CO_2 for 2 h prior to cell seeding. Next, PC12 cells were seeded at a density of 5x10^4 cells/cm^2 in 600 ml of RPMI in each well. Two hours later, NGF-CG or NGF-FC scaffold (2 x 2 cm) was placed perpendicularly into the center cavity. Cells on TCPS were used as the controls. Two hundred ng/ml of NGF in soluble format was added into the positive control and the negative control received no NGF. After 4 days, cells were fixed with 10% formalin, permeabilized with 0.05% Triton-X with 50 mM glycine in PBS, and stained with DAPI (1:1000) and phalloidin-oregon green (1:200) for nuclei and actin cytoskeleton respectively. Finally, images were taken under the epi-fluorescent microscope. The number of cells bearing neurite outgrowth longer than twice the cell body length from 4 different areas of each coverslip was quantified (n > 1000). The study was done in triplicates.

4.2.3.6 Direct PC12 cell culture experiment

NGF-CG, NGF-FC, and BSA-FC scaffolds (as control) were cut to 24-well size and coated with collagen type IV (50 μg/cm^2) for 1 h. Thereafter, the scaffolds were washed twice with sterile PBS and equilibrated in serum free RPMI for 15 min at

37°C, 5% CO_2 prior to cell seeding. PC12 cells were seeded at $5x10^4$ cells/cm^2 in 1 ml of serum free RPMI. For NGF-CG scaffolds, cells were divided into two groups - cells seeded onto the surface with higher NGF concentration (denoted as NGF-CG Side 1, Figure 2b) and cells seeded onto the opposite surface with lower NGF concentration (denoted as NGF-CG Side 2, Figure 2b). The experimental controls comprised of cells seeded on BSA-FC scaffolds. Specifically, the positive control received 200 ng/ml of NGF supplementation whilst the negative control received serum free RPMI only.

On day 4, cells were fixed and stained for nuclei and actin (phalloidin Alexafluor 633 at 1:200 dilution) following the same protocol as the underagarose assay. The scaffolds were then analyzed using confocal microscopy (Zeiss LSM-710). Z-stack confocal imaging was adopted to capture neurite penetration into the scaffolds. Images were captured at an interval of 1 μm. The percentage of cells bearing neurite outgrowth was also quantified following the same criteria as the underagarose assay. The study was done in triplicates.

Cell viability on electrospun scaffolds was tested on day 4 using Live/Dead assay. Cells were incubated in live (1:2000 dilution) and dead (1:500 dilution) cell markers for 30 min prior to imaging using the epi-fluorescent microscope.

4.2.3.7 Statistical analysis

Data is presented as mean ± standard error of mean (S.E.). Unpaired student t-test was used to compare the percentage of PC12 cells with neurite outgrowth in the underagarose assay and the direct cell culture experiment. Statistical comparisons between fiber diameter and cell viability were conducted using ANOVA and Tukey post-hoc tests after verifying equal variances.

4.3 Results

4.3.1 Fiber morphology and core-shell structure evaluation

The average fiber diameters of the samples are shown in Table 4.2. No significant difference was observed. As shown in Figure 4.3a, bead-free fibers with smooth surfaces were obtained. Most fibers exhibited core-shell structures albeit the variation in shell thickness and core size (Figure 4.3b). Additionally, some fibers appeared to be uniaxial, without the desired core-shell structure.

	NGF-FC	NGF-CG	Plain (BSA-FC)	Plain (BSA-CG)
Fiber Φ (nm)	819 ± 16	832 ± 18	845 ± 15	844 ± 21

Table 4.2. Average fiber diameters of experimental samples, mean ± S.E..

4.3.2 Protein gradient visualization

Figure 4.4a shows the cross section of the FITC-BSA-CG scaffold with FITC-BSA encapsulated in a gradient manner. The gradual increase in FITC signal intensity corresponded with the increase in protein concentration throughout the thickness of the scaffold.

4.3.3 Quantification of protein gradient

Figure 4b illustrates the changes in BSA concentration with respect to time

within the core solution during electrospinning and with respect to scaffold thickness after nanofiber encapsulation. The concentration gradient of BSA within the core solution was 283 μg/ml/min (or 48 μg/ml/μm) whilst the protein gradient encapsulated within the fibers was 107 μg/ml/min (or 18 μg/ml/μm).

4.3.4 Release kinetics

Figures 4.5a and 4.5b show the release profiles of NGF and BSA respectively. Initial burst releases of 26.9 ± 0.2 % NGF and 25.6 ± 1.4 % BSA were observed. Following that, the proteins were released in a sustained manner for up to 30 and 40 days for NGF and BSA respectively. A total of 80.4 ± 3.6 % of NGF and 97.9 ± 0.9 % of BSA were detected and the experimental loading efficiencies of NGF and BSA were (24 ± 0.3) x 10^{-2} % and (14.5 ± 1.0) % respectively.

4.3.5 Underagarose assay

Figure 4.6 illustrates a significantly higher percentage of cells with neurite outgrowth when cells were in closer proximity to the surface of NGF-CG scaffolds that was endowed with a higher NGF concentration (7.1 ± 1.9 % on Side 1 vs. 0.8 ± 0.3 % on Side 2, $p < 0.05$). In contrast, no difference in cellular behavior was observed when NGF-FC scaffolds were used. When exposed to NGF-CG and NGF-FC scaffolds, the percentage of cells bearing neurite outgrowth was significantly less than the positive control ($p < 0.05$). The corresponding morphology of the cells is shown in Figure 4.6b, where green and blue represent actin cytoskeleton and cell nuclei respectively. In the absence of NGF, no neurite outgrowth was observed.

4.3.6 Direct PC12 cell culture experiment

As indicated in Figure 4.7, cell viability on all electrospun scaffolds (NGF-CG, NGF-FC and BSA-FC) was high in the presence of NGF. In these samples, a fraction of live cells beared neurite outgrowth, whilst some remained rounded but attached well onto the scaffolds. On BSA-FC scaffolds with no NGF supplementation (negative control), PC12 cells remained rounded with no observable neurite outgrowth. Concurrently, cell viability was significantly lower. For NGF-CG scaffolds, a higher percentage of cells with neurite outgrowth was observed when cells were cultured directly on the surface with higher NGF concentration. In contrast, no difference in cellular behavior was seen when NGF-FC scaffolds were used (Figure 4.8).

The corresponding Z-stack confocal images tracking neurite outgrowth direction in response to NGF chemotactic cues are shown in Figure 4.9. On NGF-CG scaffolds, although extensive neurite extensions were observed from cells cultured on the surface with higher NGF concentration (Figure 4.9a, white arrows), neurite penetration into the scaffolds was low and could be tracked within 2 to 3 Z-stack image frames. In contrast, extensive neurite extension and penetration were observed when cells were cultured on the surface with lower NGF concentration (Figure 4.9b, white arrows). In particular, neurites appeared to penetrate at least 6-8 mm deep into the scaffolds. Such extensive neurite penetration was also absent from cells on NGF-FC scaffolds (Figure 9c, white arrows). Figures 4.9a2, 4.9b2 and 4.9c2 show the final combined Z-stack series for Figures 4.9a1, 4.9b1 and 4.9c1 respectively. The white arrows indicate the full length of the neurites that were being tracked.

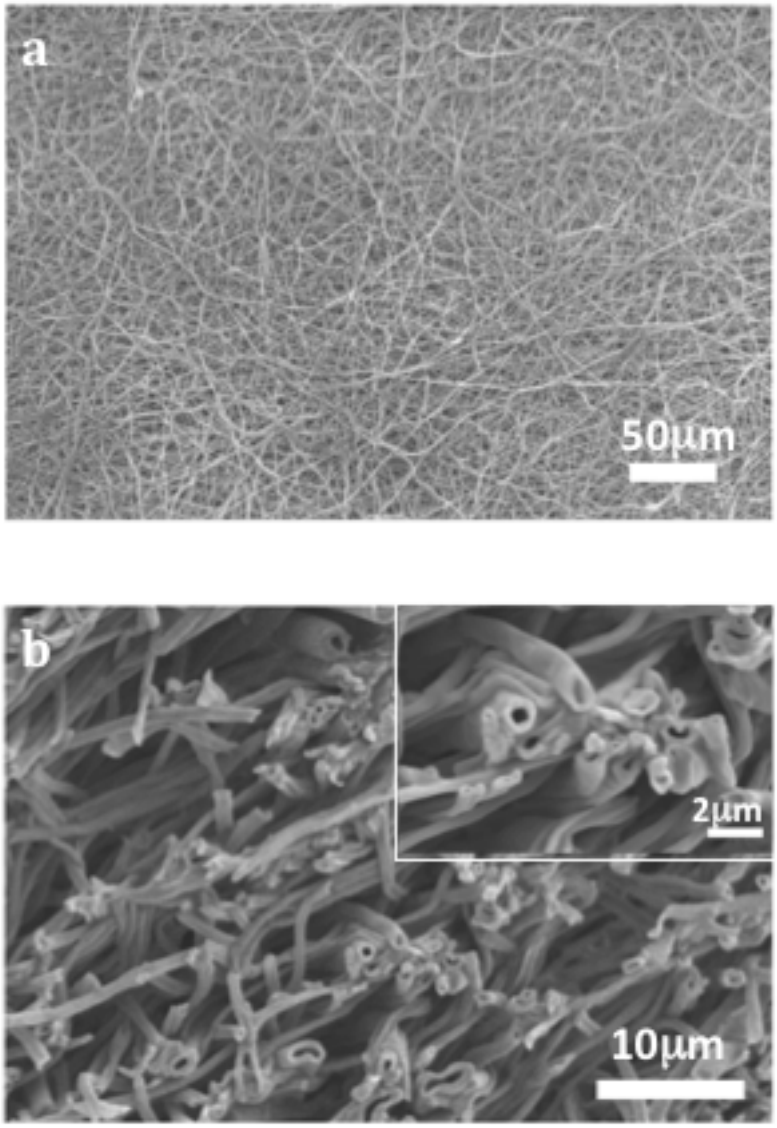

Figure 4.3. SEM micrographs of (a) overview of scaffold and (b) core-shell structure of nanofibers.

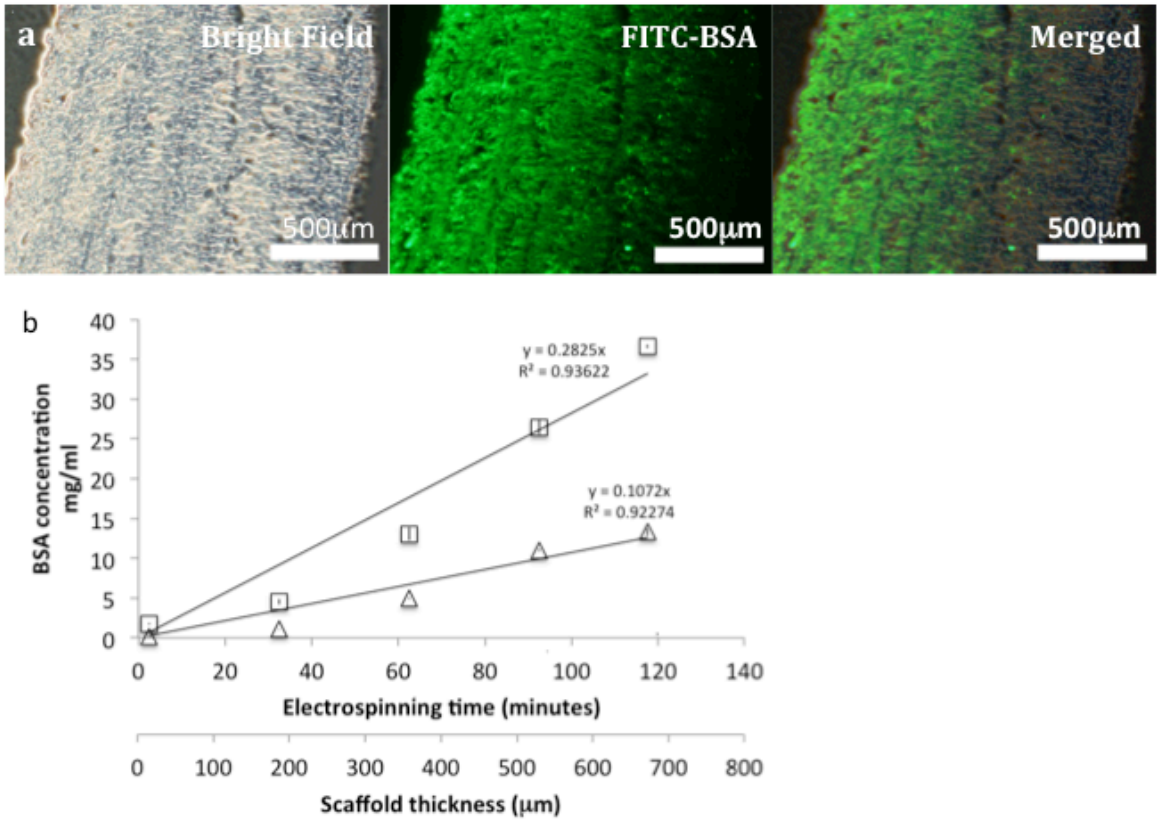

Figure 4.4. Visualization and quantification of encapsulated gradient. (a) Light and fluorescent microscopy images of cross-section of FITC-BSA-CG scaffolds revealing FITC-BSA fluorescent intensity gradient; and (b) variation of BSA concentration with respect to electrospinning time and thickness of BSA-CG scaffold. Triangle: BSA concentration within core solution during electrospinning. Square: BSA concentration extracted from BSA-CG fibers. n=3, mean ± S.E.

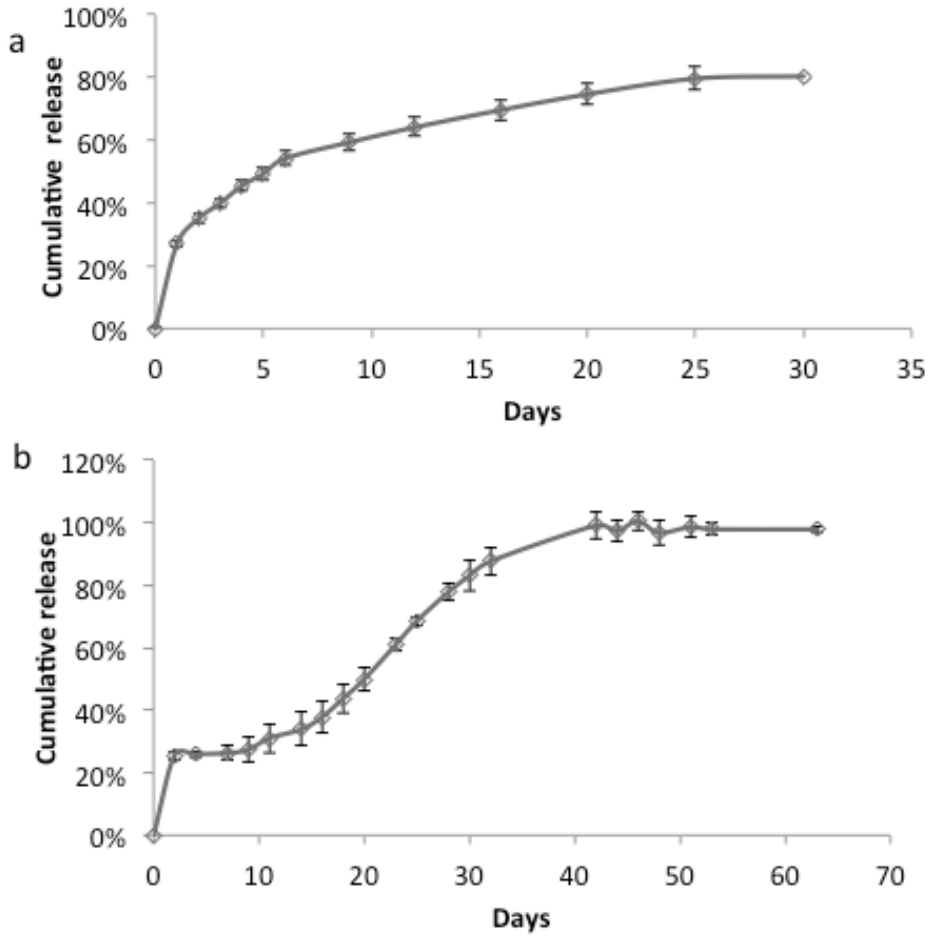

Figure 4.5. Release profiles of (a) NGF and (b) BSA from coaxial electrospun nanofibers, n=3, mean ± S.E..

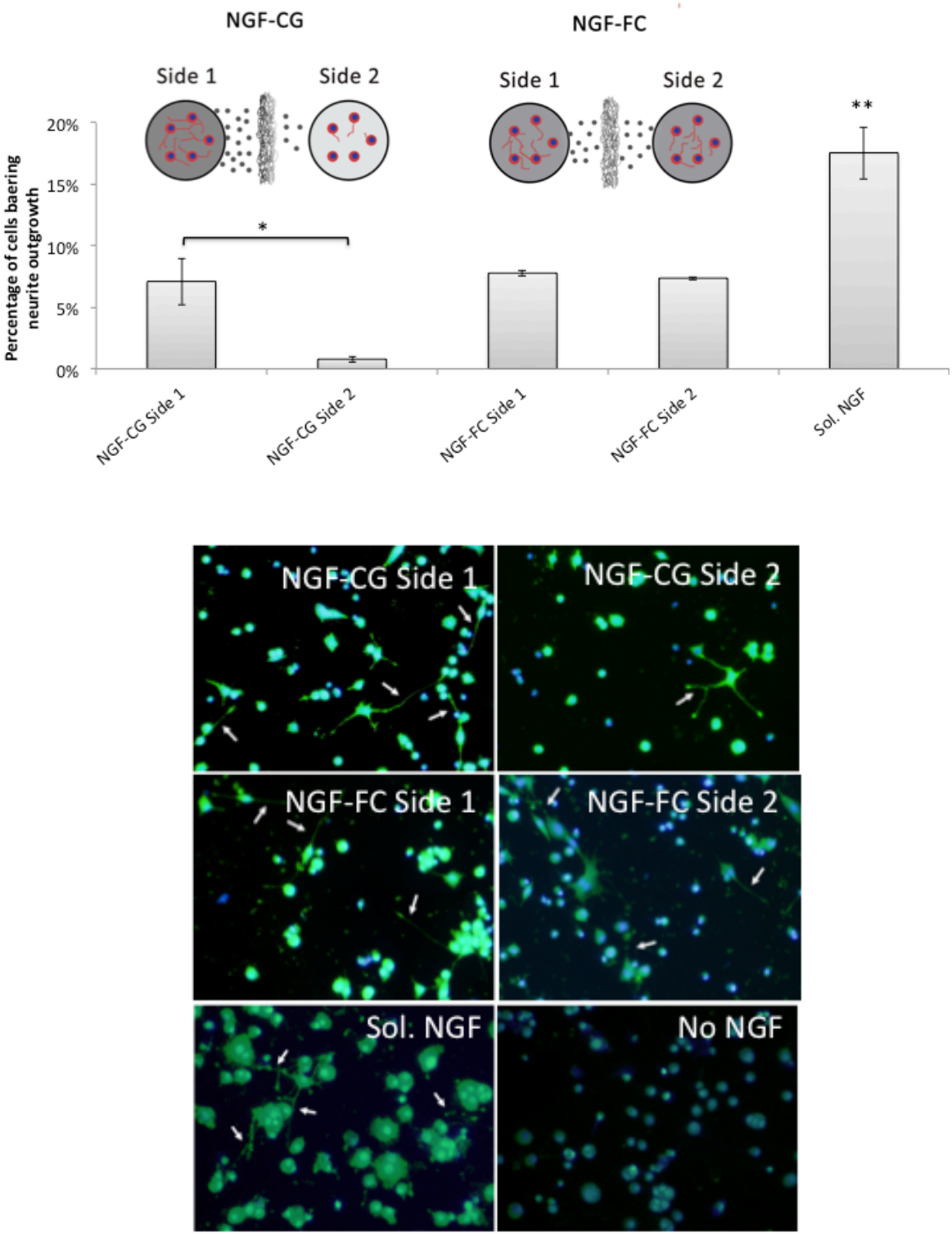

Figure 4.6. Neurite outgrowth from PC12 cells in underagarose assay. (a) Percentage of cells bearing neurite outgrowth, n=3, mean ± S. E., *: $p < 0.05$, t-test; **$p < 0.05$, ANOVA; and b) fluorescent images of PC12 cells demonstrating neurite outgrowth (white arrows) in response to NGF. Green: actin cytoskeleton; blue: nuclei.

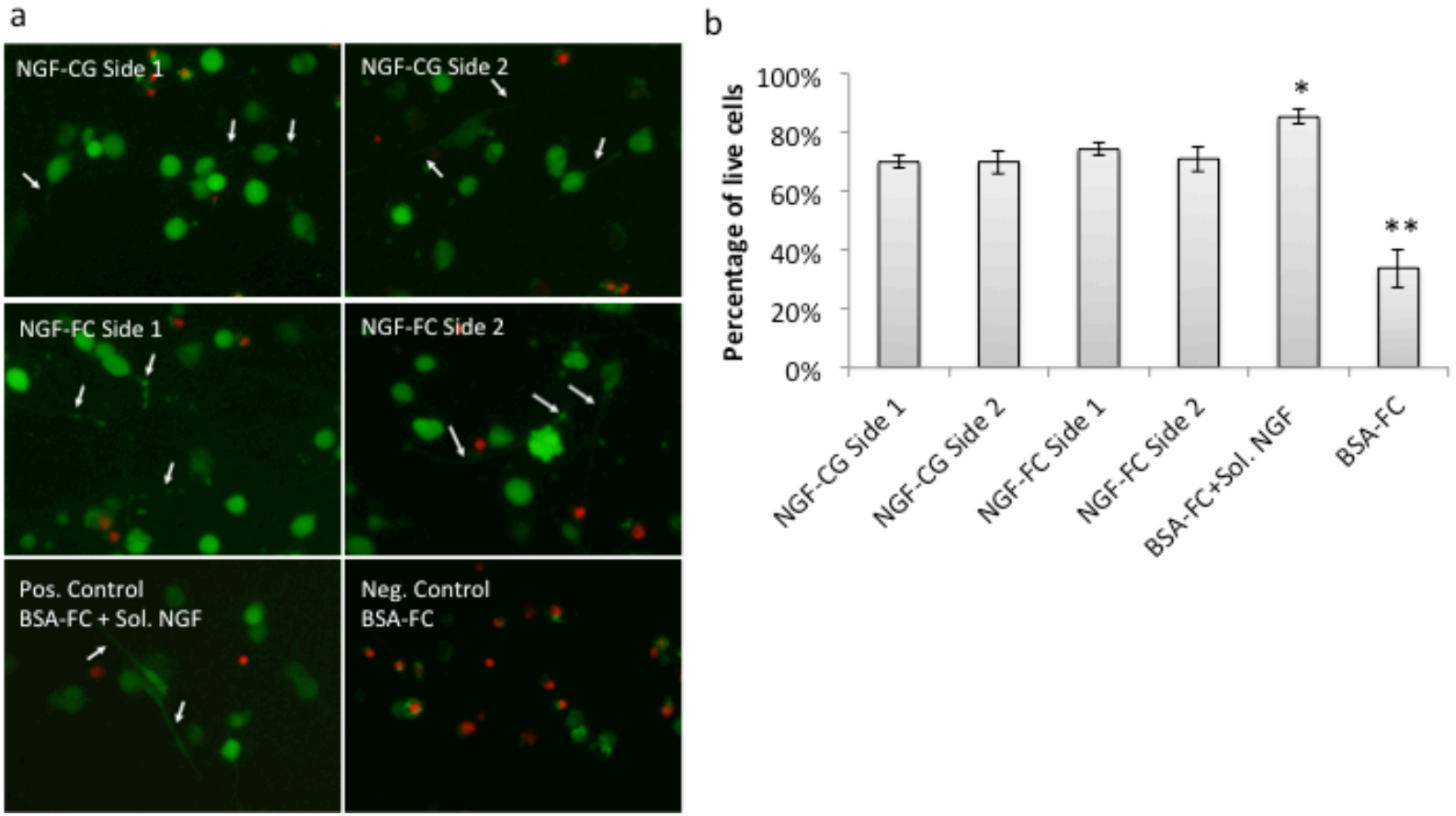

Figure 4.7. Live-dead assay of PC12 cells cultured directly on scaffolds for 4 days. (a) epifluorescence images depicting live (green) and dead (red) cells. White arrows: neurite outgrowth; and (b) percentage of live cells on scaffolds. n=3, mean ± S. E.. * and ** indicate significant difference as compared to NGF-CG and NGF-FC (p<0.05, ANOVA).

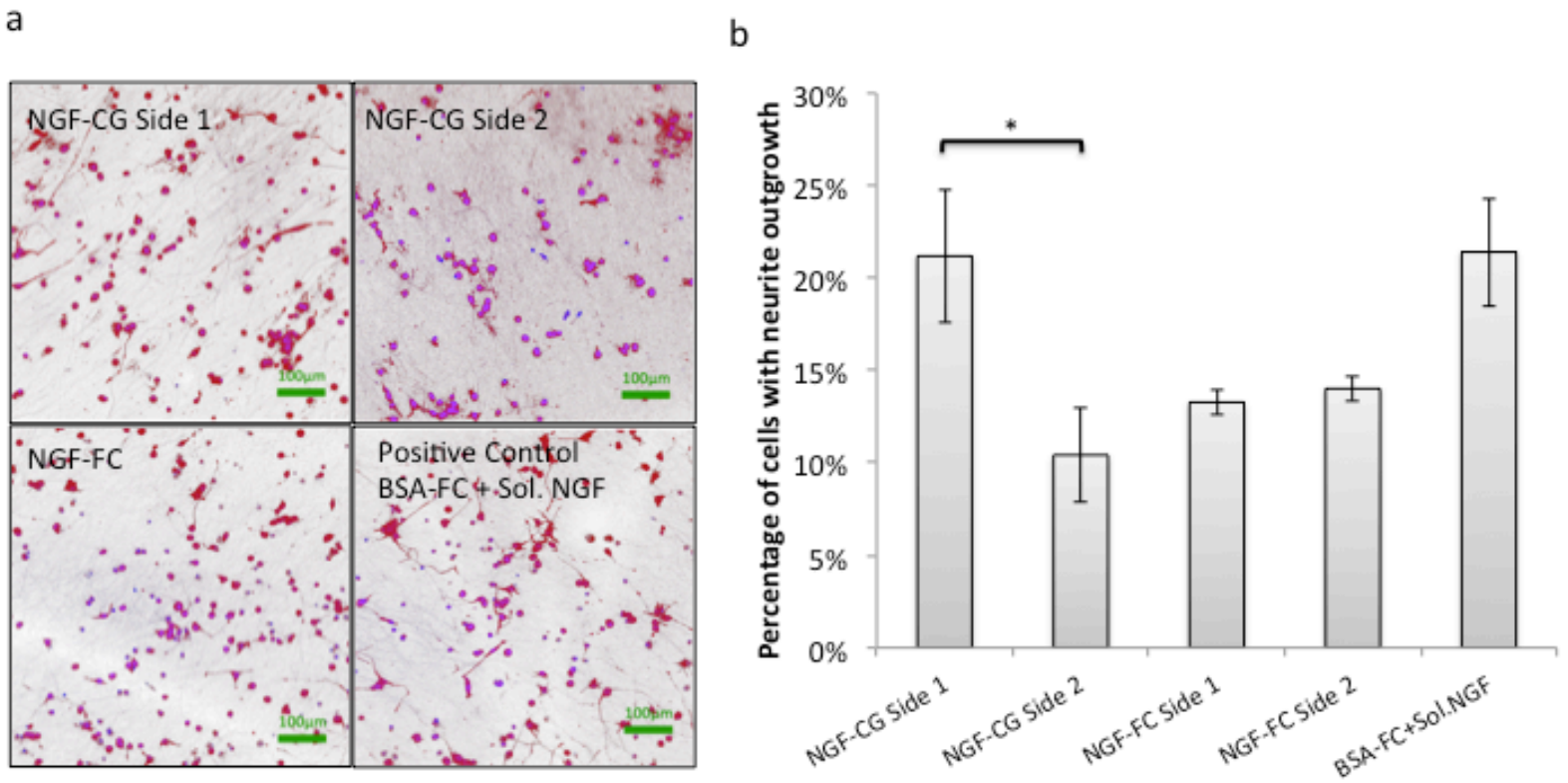

Figure 4.8. Neurite outgrowth from cells cultured directly on electrospun scaffolds. (a) Confocal images of cells in response to NGF. Red and blue signals indicate actin cytoskeleton and nuclei staining respectively; and (b) percentage of cells with neurite outgrowth. n=3, mean ± S.E., *: $p<0.05$, t-test.

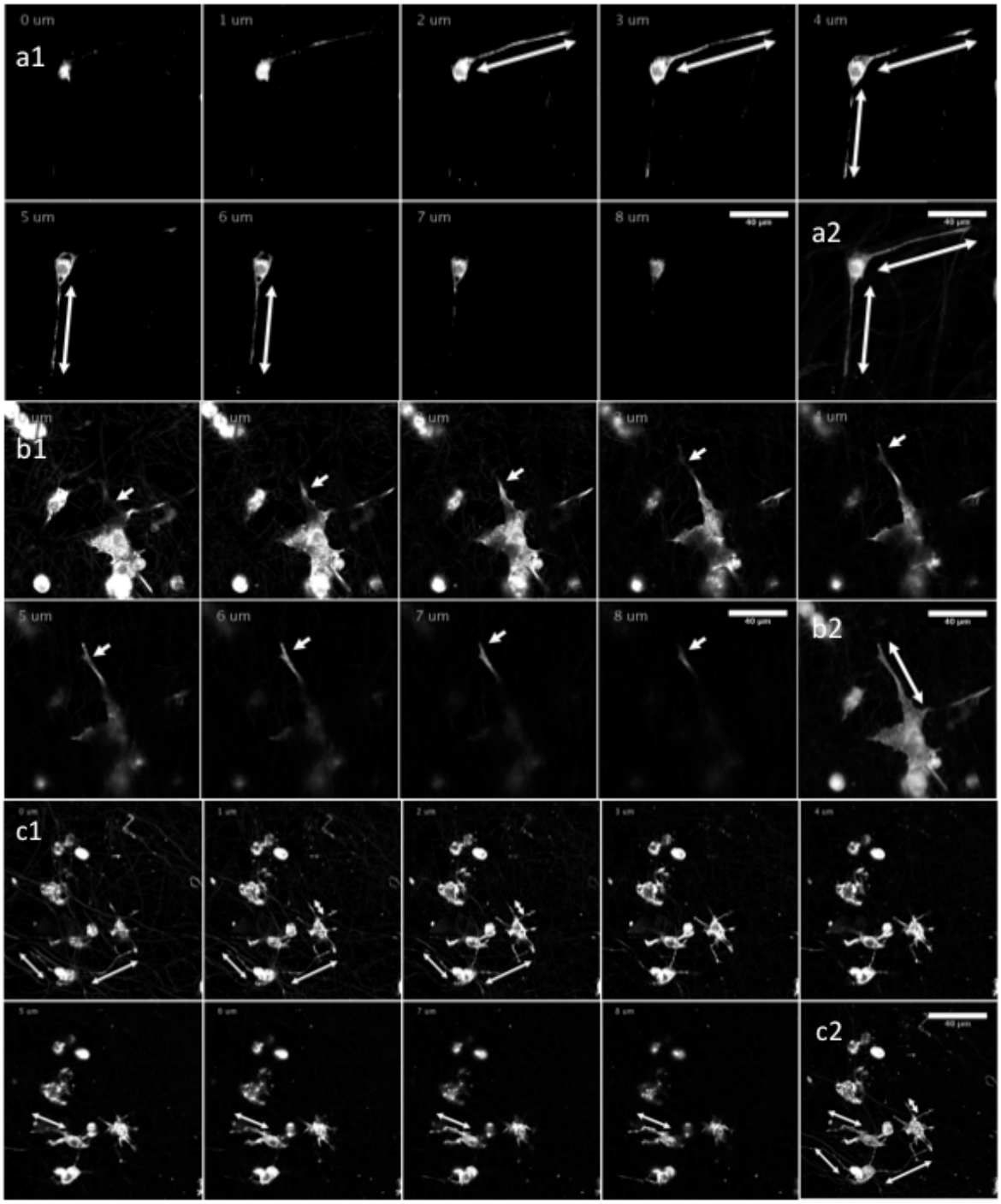

Figure 4.9. Confocal Z-stack image series (thickness =1μm) tracking PC12 neurite outgrowth on scaffolds. (a1) NGF-CG Side 1, (b1) NGF-CG Side 2, and (c1) NGF-FC. (a1 and c1) Limited neurite penetration into scaffolds was observed in cells seeded on NGF-CG Side 1 and NGF-FC, and (b1) more extensive neurite penetration spanning 8 frames (8 served in cells seeded on NGF-CG Side 1 and NGa2, b2, c2) Combined stacked images of (a1), (b1) and (c1) respectively. Scale bar: 40 0 nd (b1) more extensive nnsive nved in cells seedneurite outgrowth.

4.4 Discussion

Imparting concentration gradients of proteins during the electrospinning process presents a constant change to core solution properties such as viscosity and conductivity. This may in turn affect nanofiber properties such as diameter and drug loading efficiency. The constant fiber diameters obtained suggested that these changes were tolerated by the optimized coaxial electrospinning parameters. Fiber size affects cell fate and differentiation [181, 245, 246, 254]. Therefore, having similar mean fiber diameter and distribution across all scaffolds used in this study helped eliminate the effects of fiber size on cellular response. On the other hand, as reflected in Figure 4b, protein loading efficiency decreased with time and increasing protein concentration. Furthermore, while majority of the fibers exhibited core-shell structures, some did not. It is possible that formation of sub-jets of shell solution occurred during electrospinning [252]. The difference in charge density between the core and shell solutions and the different rate of accumulation of both solutions at the needle tips may also result in uniaxial fiber formation [121, 124]. Since the parameters used in this study are already optimized, a possible alternative to improve the system may be to further stabilize the electrospinning polymer jet by enhancing the polymer molecular weight of the shell solution.

In this study, BSA was chosen as the model protein for the quantification and visualization of protein gradient. This is because BSA is commonly used as a carrier protein to protect and stabilize labile growth factors such as NGF. To serve its purpose, BSA is typically used in much larger quantities (1-2 orders of magnitude higher) than the highly potent growth factors [105, 131, 141, 251, 255]. In this study, the concentration of BSA was 2 orders of magnitude higher than NGF. Due to the

significantly higher amount of BSA utilized, changes in BSA concentration will contribute more significantly towards any variations in the electrospinning process. By focusing on this model carrier protein, one may also easily extend and translate the optimized parameters and experimental findings to other potent growth factors. Furthermore, since BSA and NGF are miscible, the resulting protein mixture is anticipated to demonstrate similar distribution profiles as BSA alone within the core electrospinning solution and within the nanofibers. Therefore, extending from the observations made on BSA, the concentration gradient of NGF may be estimated to be 303 ng/ml/μm within the NGF-CG core solution and 115 ng/ml/μm within the NGF-CG fiber scaffolds. This concentration gradient, although 3 orders of magnitude higher than shown by previous studies (min. concentration of 133 ng/ml/mm for significant neurite guidance effect [34]) did not appear to be cytotoxic as indicated by the direct culture experiment. This is likely due to the fact that the release of NGF was limited by diffusion and the resulting concentration gradient that the cells were subjected to was lower than the encapsulated gradient. For this reason, the encapsulation of a higher concentration gradient is necessary to ensure that a minimum effective concentration gradient can be presented over a prolonged time period.

The BSA and NGF release profiles illustrate the overall average protein concentrations since the supernatants were collected in bulk for quantification. As indicated, both proteins were released in a sustained manner. The faster release rate of NGF is likely due to its smaller molecular weight of 26.3 kDa as compared to BSA (Mw: 67 kDa). The initial burst releases are likely attributed to proteins that were located near the surface of the nanofibers. This may have resulted from the possible mixing of core and shell solutions during electrospinning [121, 124, 141, 253], and this mixing is postulated to occur predominantly in the Taylor cone [125]. Increasing the

degree of immiscibility of both core and shell solutions by varying the choice of respective solvents may attenuate the mixing.

In the underagarose assay, cells that were closer to the high NGF concentration surface of NGF-CG scaffolds demonstrated more extensive neurite outgrowth. Besides illustrating the presence of a gradient of diffusible NGF, the assay also demonstrated that the NGF was at least partially bioactive and was present in a therapeutic amount for neurite outgrowth. The exact level of NGF bioactivity, unfortunately, could not be quantified due to the low sensitivity and non-linearity of the assay [45, 256-258]. Additionally, the amount of NGF present in each well does not reflect the total amount of NGF released since a portion would have remained entrapped within the agarose gel. The possible partial loss of bioactivity due to electrospinning and gel entrapment may have resulted in the smaller percentage of cells bearing neurite outgrowth in cells exposed to NGF-FC and NGF-CG scaffolds as compared to cells that received fresh soluble NGF supplementation.

The cytocompatibilty of the scaffolds and the effect of the encapsulated concentration gradient of NGF on cellular response were evaluated by culturing PC12 cells directly onto the scaffolds. Cell spreading and attachment on the fibers together with the formation of neurites in the presence of NGF indicated that the substrates were compatible with PC12 cells. The presence of NGF was critical in maintaining PC12 cell survival in the absence of serum as cells cultured in the absence of NGF exhibited significantly lower viability (Figure 4.7). Supplementation of fresh soluble NGF enhanced cell viability significantly (Figure 4.7, positive control vs NGF-FC and NGF-CG). This may be due to the partial loss of bioactivity in electrospun NGF. However, this difference in cellular behavior became less significant in terms of neurite outgrowth (Figure 4.8, NGF-CG Side 1 vs. positive control).

The neurite outgrowth on nanofibrous scaffolds was tracked by using Z-stack confocal imaging. Analyses of PC12 cells seeded on the high NGF concentration surface of NGF-CG substrates showed that in most cases, the entire length of neurite extensions could be tracked within two to three frames of imaging, i.e. 2-3 microns deep (Figure 4.9a). Similar outcome was observed when cells were cultured on either surface of NGF-FC scaffolds. These results suggested a lack of neurite penetration and that most neurite extensions were two-dimensional. In contrast, when cells were cultured on the low NGF concentration surface of NGF-CG scaffolds, neurite outgrowth extended several microns deep into the scaffold. As indicated in Figure 4.9b, the typical penetration depth of about 6-8 μm translates to about 7-10 layers of nanofibers deep.

Although we did observe some neurite penetration on the low NGF concentration surface, the preferential direction towards the positive NGF gradient appears to be less perpendicular than expected. The adoption of static culture in this study may be a possible reason. In static culture, the establishment of equilibrium NGF concentration over time may have dampened the effect of the protein gradient. Loss of chemotactic cues can profoundly affect neurite outgrowth directionality since neurite growth tips are very sensitive to changes in concentrations of diffusible factors. The turning, extension and retraction of growth cones upon the removal of neurotrophic factors can occur in a matter of minutes [30, 46, 49]. The choice of a 4-day evaluation time point for PC12 assays stems from this possible establishment of NGF equilibrium concentration and also from the fact that this time point is frequently adopted for PC12 neurite outgrowth assay [45, 259-262]. Further studies involving the use of these scaffolds under dynamic culture conditions or *in vivo* implantation will be undertaken and are anticipated to result in more drastic differences in neurite penetration depths.

This is because while *in vitro* cellular penetration into electrospun substrates have been poor due to pore size limitations [129, 263, 264], complete cell infiltration of electrospun scaffolds have been observed in as early as one week under *in vivo* conditions [265-267].

Electrospun nanofibers reduce fibrous capsule formation and promote tissue-implant integration [265]. Combined with concentration gradients of neurotrophic factors, these substrates may find useful applications as novel coatings for neural electrode implants. Currently, the implantation of neural electrodes is plagued by many problems ranging from inflammatory response, gliosis to loss of neurons at the electrode-tissue interface. These factors can lead to implant isolation, loss of signal and, ultimately, implant failure. Electrospun fibers have been used to improve the biocompatibility of neural electrodes. [248-250]. It is, therefore, possible that the synergistic effects of encapsulating concentration gradients of neurotrophic factors provide a sustained availability of neuroprotective agents and direct neurite penetration towards neural electrodes for enhanced tissue-implant integration and signal transduction. On basic science, these biomimicking substrates can also serve as novel scaffolds for understanding many fundamental questions related to cell chemotaxis in a three-dimensional ECM-like microenvironment.

4.5 Conclusion

Altogether, a method of incorporating concentration gradient of diffusible NGF into electrospun nanofibrous scaffolds was established. The experimental results demonstrate the presence of an encapsulated protein gradient throughout the thickness of the electrospun scaffolds. In particular, the underagarose-PC12 assay demonstrated

the effect of the NGF concentration gradient over a wider range via diffusion and the direct culture of PC12 cells showed neurite-scaffold interaction in response to the localized concentration of diffusible NGF gradient. The combination of topographical cues, sustained delivery of bioactive chemicals presented in a concentration gradient format within a single scaffold may find potential applications in regenerative medicine, especially where chemotactic signals are required for regulating cell fate.

5 Conclusion and future directions

Adopting chemotactic concentration gradient into implantable scaffolds opens up many benefits that so far limited only to *in vitro* platform. This project aimed at developing methods to integrate such concentration gradient into electrospun fibers. The resulting scaffold features ECM mimicking topography and sustained delivery of bioactive chemicals on top of the availability of chemotactic concentration gradient for extended period. The versatility in varying these factors would allow more flexibility and control in modulating cell fate and behavior.

Firstly we attempted to solve the major problem hindering the effort in imparting chemotactic concentration gradient into gelatin nanofibers, that is the crosslinking. The use of enzymatic crosslinking by mTG was pursued based on its many merits, notably its biodegradability and low toxicity. We have shown that fibers with encapsulated mTG, upon provision of moisture, underwent crosslinking *in situ* albeit only to a limited degree. With supplemental crosslinking, the fibers could last for at least 7 days at physiological condition with retained fibrous structure for the majority. Even so, the result and the crosslinking procedures were not good enough and appropriate to enable the inclusion of diffusible bioactive chemicals and its concentration gradient. There are many factors that should be further investigated in order to improve the crosslinking method and characterize the scaffold. With the proposed use of higher specific activity mTG, we expect that the efficiency of the *in situ* crosslinking can be improved dramatically. A break from the reliance of additional crosslinking in mTG solution would be highly advantageous, especially for the encapsulation of diffusible bioactive chemicals and their concentration gradient. On the other hand, use of synthetic

materials is more straightforward. We have successfully established a method of conferring chemotactic concentration gradient into fibers made of PCL and PEG by coaxial electrospinning. The existence of endowed concentration was verified and with the use of PC12 cells, the bioactivity of released NGF and the effect of concentration gradient on their neurite outgrowth were exhibited.

There are many fronts that electrospun fibrous scaffold featuring concentration gradient may find use. 1) This biomimetic scaffold, together with the use of dynamic *in vitro* culture, can serve as a platform to study cell response to chemotactic concentration gradient in a more physiologically relevant setup. Not limited to only one concentration gradient, multiple concentration gradients with different steepness and different trend could be incorporated with the established method easily. It is also a subject of great interest to look at the effect of concentration gradient to *in vitro* stem cells differentiation. 2) Chemotactic cues may improve cell penetration into electrospun scaffold *in vitro*. In typical culture setup, cells seeded tend to stay on the surface without pronounced penetration [129, 263, 264]. This is unfavorable as it makes the creation of 3D cellular construct with electrospun fibers *ex vivo* impractical. 3) Inclusion of chemotactic concentration gradient into *in vivo* implants can be used to augment the current strategy in many regenerative efforts. Other than directing neurites to facilitate neurons interaction with neural electrodes and during renervation, angiogenesis, cell homing, migration of cells towards specific area like wounded location, are some other areas that would be interesting to look at. [1-8].

6 References

1. Wu, W., et al., *Directional guidance of neuronal migration in the olfactory system by the protein Slit.* Nature, 1999. **400**(6742): p. 331-336.
2. Chen, J., et al., *The attractive effects of nerve regeneration chamber fluid and degenerated nerve segments on the growth and the migration of the cocultured dorsal root ganglion neuron.* Zhonghua wai ke za zhi [Chinese journal of surgery], 2000. **38**(3): p. 208-211, 12.
3. Ward, M.E., H. Jiang, and Y. Rao, *Regulated formation and selection of neuronal processes underlie directional guidance of neuronal migration.* Molecular and Cellular Neuroscience, 2005. **30**(3): p. 378-387.
4. Baker, R.E. and P.K. Maini, *Travelling gradients in interacting morphogen systems.* Mathematical Biosciences, 2007. **209**(1): p. 30-50.
5. Carmona-Fontaine, C., H. Matthews, and R. Mayor, *Directional cell migration in vivo: Wnt at the crest.* Cell adhesion & migration, 2008. **2**(4): p. 240-242.
6. Mishra, A., et al., *Homing of Cancer Cells to the Bone.* Cancer Microenvironment, 2011: p. 1-15.
7. Roussos, E.T., J.S. Condeelis, and A. Patsialou, *Chemotaxis in cancer.* Nature Reviews Cancer, 2011. **11**(8): p. 573-587.
8. Zantl, R. and E. Horn, *Chemotaxis of slow migrating mammalian cells analysed by video microscopy*, 2011. p. 191-203.
9. Baier, H. and F. Bonhoeffer, *Axon guidance by gradients of a target-derived component.* Science, 1992. **255**(5043): p. 472-475.
10. Sun, Q.L., et al., *Growth cone steering by receptor tyrosine phosphatase Œ¥ defines a distinct class of guidance cue.* Molecular and Cellular Neuroscience, 2000. **16**(5): p. 686-695.
11. Baker, K.A., et al., *When a diffusible axon guidance cue stops diffusing: roles for netrins in adhesion and morphogenesis.* Current Opinion in Neurobiology, 2006. **16**(5): p. 529-534.
12. Cao, X. and M.S. Shoichet, *Investigating the synergistic effect of combined neurotrophic factor concentration gradients to guide axonal growth.* Neuroscience, 2003. **122**(2): p. 381-9.
13. Charron, F. and M. Tessier-Lavigne, *Novel brain wiring functions for classical morphogens: A role as graded positional cues in axon guidance.* Development, 2005. **132**(10): p. 2251-2262.
14. Solowska, J.M., et al., *Pontocerebellar axon guidance: Neuropilin-1-and semaphorin 3A-sensitivity gradients across basilar pontine nuclei and semaphorin 3A variation across cerebellum.* Molecular and Cellular Neuroscience, 2002. **21**(2): p. 266-284.
15. Tessier-Lavigne, M. and M. Placzek, *Target attraction: Are developing axons guided by chemotropism?* Trends in Neurosciences, 1991. **14**(7): p. 303-310.
16. Zheng, M. and D.P. Kuffler, *Guidance of regenerating motor axons in vivo by gradients of diffusible peripheral nerve-derived factors.* Journal of Neurobiology, 2000. **42**(2): p. 212-219.
17. Zhang, Y., et al., *Cell adhesion molecules of the immunoglobulin superfamily in axonal regeneration and neural repair.* Restor Neurol Neurosci, 2008. **26**(2-3): p. 81-96.

18. Astic, L., et al., *Expression of netrin-1 and netrin-1 receptor, DCC, in the rat olfactory nerve pathway during development and axonal regeneration.* Neuroscience, 2002. **109**(4): p. 643-56.
19. Chisholm, A. and M. Tessier-Lavigne, *Conservation and divergence of axon guidance mechanisms.* Current Opinion in Neurobiology, 1999. **9**(5): p. 603-15.
20. Kennedy, T.E., *Cellular mechanisms of netrin function: long-range and short-range actions.* Biochemistry and cell biology = Biochimie et biologie cellulaire, 2000. **78**(5): p. 569-75.
21. Wang, K.H., et al., *Biochemical purification of a mammalian slit protein as a positive regulator of sensory axon elongation and branching.* Cell, 1999. **96**(6): p. 771-784.
22. Li, H.S., et al., *Vertebrate slit, a secreted ligand for the transmembrane protein roundabout, is a repellent for olfactory bulb axons.* Cell, 1999. **96**(6): p. 807-818.
23. KIRYUSHKO, D., V. BEREZIN, and E. BOCK, *Regulators of Neurite Outgrowth: Role of Cell Adhesion Molecules.* Annals of the New York Academy of Sciences, 2004. **1014**(Gastroenteropancreatic Neuroendocrine Tumor Disease: Molecular and Cell Biological Aspects): p. 140-154.
24. Colavita, A. and J.G. Culotti, *Suppressors of ectopic UNC-5 growth cone steering identify eight genes involved in axon guidance in Caenorhabditis elegans.* Developmental Biology, 1998. **194**(1): p. 72-85.
25. Zheng, J.Q., et al., *Turning of nerve growth cones induced by neurotransmitters.* Nature, 1994. **368**(6467): p. 140-4.
26. Jarjour, A.A., et al., *Netrin-1 is a chemorepellent for oligodendrocyte precursor cells in the embryonic spinal cord.* Journal of Neuroscience, 2003. **23**(9): p. 3735-3744.
27. Tojima, T., et al., *Second messengers and membrane trafficking direct and organize growth cone steering.* Nature Reviews Neuroscience, 2011. **12**(4): p. 191-203.
28. Song, H.J. and M.M. Poo, *The cell biology of neuronal navigation.* Nature Cell Biology, 2001. **3**(3): p. E81-E88.
29. Akiyama, H., et al., *Control of Neuronal Growth Cone Navigation by Asymmetric Inositol 1,4,5-Trisphosphate Signals.* Science Signaling, 2009. **2**(79): p. -.
30. Gundersen, R.W. and J.N. Barrett, *Neuronal chemotaxis: Chick dorsal-root axons turn toward high concentrations of nerve growth factor.* Science, 1979. **206**(4422): p. 1079-1080.
31. Wu, K.Y., et al., *Local translation of RhoA regulates growth cone collapse.* Nature, 2005. **436**(7053): p. 1020-1024.
32. Leung, K.M., et al., *Asymmetrical beta-actin mRNA translation in growth cones mediates attractive turning to netrin-1.* Nature Neuroscience, 2006. **9**(10): p. 1247-1256.
33. Hengst, U., et al., *Axonal elongation triggered by stimulus-induced local translation of a polarity complex protein.* Nature Cell Biology, 2009. **11**(8): p. 1024-U263.
34. Cao, X. and M.S. Shoichet, *Defining the concentration gradient of nerve growth factor for guided neurite outgrowth.* Neuroscience, 2001. **103**(3): p. 831-840.
35. Chao, M.V., *Neurotrophin receptors: A window into neuronal differentiation.* Neuron, 1992. **9**(4): p. 583-593.

36. Skup, M.H., *BDNF and NT-3 widen the scope of neurotrophin activity: Pharmacological implications.* Acta Neurobiologiae Experimentalis, 1994. **54**(2): p. 81-94.
37. Narhi, L.O., et al., *Comparison of the biophysical characteristics of human brain-derived neurotrophic factor, neurotrophin-3, and nerve growth factor.* Journal of Biological Chemistry, 1993. **268**(18): p. 13309-13317.
38. Lu, B., P.T. Pang, and N.H. Woo, *The yin and yang of neurotrophin action.* Nature Reviews Neuroscience, 2005. **6**(8): p. 603-614.
39. Sendtner, M., et al., *Developmental motoneuron cell death and neurotrophic factors.* Cell and Tissue Research, 2000. **301**(1): p. 71-84.
40. Casaccia-Bonnefil, P., C. Gu, and M.V. Chao, *Neurotrophins in cell survival/death decisions.* The Functional Roles of Glial Cells in Health and Disease, 1999. **468**: p. 275-282.
41. Pehar, M., et al., *Astrocytic production of nerve growth factor in motor neuron apoptosis: implications for amyotrophic lateral sclerosis.* Journal of Neurochemistry, 2004. **89**(2): p. 464-73.
42. Wong, V., et al., *The neurotrophins BDNF, NT-3 and NT-4/5, but not NGF, up-regulate the cholinergic phenotype of developing motor neurons.* European Journal of Neuroscience, 1993. **5**(5): p. 466-474.
43. Hu, X., et al., *Sensory axon targeting is increased by NGF gene therapy within the lesioned adult femoral nerve.* Experimental Neurology, 2010. **223**(1): p. 153-165.
44. Ockel, M., G.R. Lewin, and Y.A. Barde, *In vivo effects of neurotrophin-3 during sensory neurogenesis.* Development, 1996. **122**(1): p. 301-307.
45. Greene, L.A., *Nerve growth factor prevents the death and stimulates the neuronal differentiation of clonal PC12 pheochromocytoma cells in serum-free medium.* J Cell Biol, 1978. **78**(3): p. 747-55.
46. Sano, M. and M. Iwanaga, *Local sprouting of neurites from cultured PC12D cells in response to a concentration gradient of nerve growth factor.* Brain Res, 1994. **656**(1): p. 210-4.
47. Kapur, T.A. and M.S. Shoichet, *Immobilized concentration gradients of nerve growth factor guide neurite outgrowth.* Journal of biomedical materials research. Part A, 2004. **68**(2): p. 235-43.
48. Li, B., et al., *A technique for preparing protein gradients on polymeric surfaces: effects on PC12 pheochromocytoma cells.* Biomaterials, 2005. **26**(13): p. 1487-95.
49. Gundersen, R.W. and J.N. Barrett, *Characterization of the turning response of dorsal root neurites toward nerve growth factor.* J Cell Biol, 1980. **87**(3 Pt 1): p. 546-54.
50. Letourneau, P.C., *Chemotactic response of nerve fiber elongation to nerve growth factor.* Developmental Biology, 1978. **66**(1): p. 183-196.
51. Bhattacharjee, N., N. Li, and A. Folch. *A neuron-benign microfluidic gradient generator for studying the growth of mammalian neurons towards axon guidance factors*. 2009.
52. Park, J.Y., et al., *Differentiation of neural progenitor cells in a microfluidic chip-generated cytokine gradient.* Stem Cells, 2009. **27**(11): p. 2646-2654.
53. Joanne Wang, C., et al., *A microfluidics-based turning assay reveals complex growth cone responses to integrated gradients of substrate-bound ECM molecules and diffusible guidance cues.* Lab on a Chip, 2008. **8**(2): p. 227-237.

54. Yu, L.M.Y., F.D. Miller, and M.S. Shoichet, *The use of immobilized neurotrophins to support neuron survival and guide nerve fiber growth in compartmentalized chambers.* Biomaterials, 2010. **31**(27): p. 6987-6999.
55. Moore, K., M. Macsween, and M. Shoichet, *Immobilized concentration gradients of neurotrophic factors guide neurite outgrowth of primary neurons in macroporous scaffolds.* Tissue Engineering, 2006. **12**(2): p. 267-278.
56. Kapur, T.A. and M.S. Schoichet, *Chemically-bound nerve growth factor for neural tissue engineering applications.* Journal of Biomaterials Science, Polymer Edition, 2003. **14**(4): p. 383-394.
57. Knapp, D.M., E.F. Helou, and R.T. Tranquillo, *A fibrin or collagen gel assay for tissue cell chemotaxis: Assessment of fibroblast chemotaxis to GRGDSP.* Experimental Cell Research, 1999. **247**(2): p. 543-553.
58. Song, H.J., G.L. Ming, and M.M. Poo, *CAMP-induced switching in turning direction of nerve growth cones.* Nature, 1997. **388**(6639): p. 275-279.
59. Sundararaghavan, H.G. and J.A. Burdick, *Gradients with depth in electrospun fibrous scaffolds for directed cell behavior.* Biomacromolecules, 2011. **12**(6): p. 2344-2350.
60. Kothapalli, C.R., et al., *A high-throughput microfluidic assay to study neurite response to growth factor gradients.* Lab on a Chip, 2011. **11**(3): p. 497-507.
61. Kim, S., H.J. Kim, and N.L. Jeon, *Biological applications of microfluidic gradient devices.* Integrative Biology, 2010. **2**(11-12): p. 584-603.
62. Miller, E.D., et al., *Inkjet printing of growth factor concentration gradients and combinatorial arrays immobilized on biologically-relevant substrates.* Combinatorial chemistry & high throughput screening, 2009. **12**(6): p. 604-18.
63. Cai, K., et al., *Inkjet printing of laminin gradient to investigate endothelial cellular alignment.* Colloids and surfaces. B, Biointerfaces, 2009. **72**(2): p. 230-5.
64. Valmikinathan, C.M., et al., *Magnetically induced protein gradients on electrospun nanofibers.* Combinatorial Chemistry and High Throughput Screening, 2009. **12**(7): p. 656-663.
65. Shi, J., et al., *Incorporating protein gradient into electrospun nanofibers as scaffolds for tissue engineering.* ACS Applied Materials and Interfaces, 2010. **2**(4): p. 1025-1030.
66. Roam, J.L., et al., *The formation of protein concentration gradients mediated by density differences of poly(ethylene glycol) microspheres.* Biomaterials, 2010. **31**(33): p. 8642-8650.
67. Wang, X., et al., *Growth factor gradients via microsphere delivery in biopolymer scaffolds for osteochondral tissue engineering.* Journal of controlled release : official journal of the Controlled Release Society, 2009. **134**(2): p. 81-90.
68. Reneker, D.H. and T. Han. *Electrical bending and mechanical buckling instabilities in electrospinning jets*. 2006.
69. Reneker, D.H. and A.L. Yarin, *Electrospinning jets and polymer nanofibers.* Polymer, 2008. **49**(10): p. 2387-2425.
70. Reneker, D.H., et al., *Bending instability of electrically charged liquid jets of polymer solutions in electrospinning.* Journal of Applied Physics, 2000. **87**(9 I): p. 4531-4547.
71. Yarin, A.L., S. Koombhongse, and D.H. Reneker, *Bending instability in electrospinning of nanofibers.* Journal of Applied Physics, 2001. **89**(5): p. 3018-3026.

72. Chew, S.Y., et al., *The role of electrospinning in the emerging field of nanomedicine.* Current pharmaceutical design, 2006. **12**(36): p. 4751-70.
73. Amiraliyan, N., M. Nouri, and M.H. Kish, *Effects of Some Electrospinning Parameters on Morphology of Natural Silk-Based Nanofibers.* Journal of Applied Polymer Science, 2009. **113**(1): p. 226-234.
74. Beachley, V. and X. Wen, *Effect of electrospinning parameters on the nanofiber diameter and length.* Materials science & engineering. C, Materials for biological applications, 2009. **29**(3): p. 663-668.
75. Skotak, M., et al., *Electrospun cross-linked gelatin fibers with controlled diameter: The effect of matrix stiffness on proliferative and biosynthetic activity of chondrocytes cultured in vitro.* Journal of Biomedical Materials Research - Part A, 2010. **95**(3 A): p. 828-836.
76. Zhang, S., et al., *Gelatin nanofibrous membrane fabricated by electrospinning of aqueous gelatin solution for guided tissue regeneration.* J Biomed Mater Res A, 2009. **90**(3): p. 671-9.
77. Songchotikunpan, P., J. Tattiyakul, and P. Supaphol, *Extraction and electrospinning of gelatin from fish skin.* Int J Biol Macromol, 2008. **42**(3): p. 247-55.
78. Zhang, Y., et al., *Electrospinning of gelatin fibers and gelatin/PCL composite fibrous scaffolds.* J Biomed Mater Res B Appl Biomater, 2005. **72**(1): p. 156-65.
79. Schiffman, J.D. and C.L. Schauer, *One-step electrospinning of cross-linked chitosan fibers.* Biomacromolecules, 2007. **8**(9): p. 2665-7.
80. Gu, S.Y., et al., *Electrospinning of gelatin and gelatin/poly(l-lactide) blend and its characteristics for wound dressing.* Materials Science and Engineering C, 2009. **29**(6): p. 1822-1828.
81. Geng, X., O.H. Kwon, and J. Jang, *Electrospinning of chitosan dissolved in concentrated acetic acid solution.* Biomaterials, 2005. **26**(27): p. 5427-32.
82. Lee, K.Y., et al., *Electrospinning of polysaccharides for regenerative medicine.* Adv Drug Deliv Rev, 2009. **61**(12): p. 1020-32.
83. Alborzi, S., L.T. Lim, and Y. Kakuda, *Electrospinning of sodium alginate-pectin ultrafine fibers.* J Food Sci, 2010. **75**(1): p. C100-7.
84. Shi, L., C. Le Visage, and S.Y. Chew, *Long-term stabilization of polysaccharide electrospun fibres by in situ cross-linking.* Journal of biomaterials science. Polymer edition, 2011. **22**(11): p. 1459-72.
85. Zhou, J., C. Cao, and X. Ma, *A novel three-dimensional tubular scaffold prepared from silk fibroin by electrospinning.* Int J Biol Macromol, 2009. **45**(5): p. 504-10.
86. Min, B.M., et al., *Electrospinning of silk fibroin nanofibers and its effect on the adhesion and spreading of normal human keratinocytes and fibroblasts in vitro.* Biomaterials, 2004. **25**(7-8): p. 1289-97.
87. Sell, S.A., et al., *Electrospinning of collagen/biopolymers for regenerative medicine and cardiovascular tissue engineering.* Adv Drug Deliv Rev, 2009. **61**(12): p. 1007-19.
88. Zhong, S., et al., *An aligned nanofibrous collagen scaffold by electrospinning and its effects on in vitro fibroblast culture.* J Biomed Mater Res A, 2006. **79**(3): p. 456-63.
89. Matthews, J.A., et al., *Electrospinning of collagen nanofibers.* Biomacromolecules, 2002. **3**(2): p. 232-8.

90. Boland, E.D., et al., *Electrospinning collagen and elastin: preliminary vascular tissue engineering.* Front Biosci, 2004. **9**: p. 1422-32.
91. Liu, T., et al., *Photochemical crosslinked electrospun collagen nanofibers: Synthesis, characterization and neural stem cell interactions.* Journal of Biomedical Materials Research Part A, 2010. **95A**(1): p. 276-282.
92. Sindelar, T., et al., *Electrospinning of fibrinogen nanofibers.* Cytotherapy, 2006. **8**: p. 45-45.
93. Wnek, G.E., et al., *Electrospinning of nanofiber fibrinogen structures.* Nano Letters, 2003. **3**(2): p. 213-216.
94. Xu, F., et al., *Improvement of cytocompatibility of electrospinning PLLA microfibers by blending PVP.* J Mater Sci Mater Med, 2009. **20**(6): p. 1331-8.
95. Carletti, E., et al., *Production of PDLA and PLGA scaffolds by microfabrication and electrospinning techniques.* Tissue Engineering Part A, 2008. **14**(5): p. 771-771.
96. Dong, C., et al., *Preparation of PVA/PEI ultra-fine fibers and their composite membrane with PLA by electrospinning.* J Biomater Sci Polym Ed, 2006. **17**(6): p. 631-43.
97. Boland, E.D., et al., *Tailoring tissue engineering scaffolds using electrostatic processing techniques: A study of poly(glycolic acid) electrospinning.* Journal of Macromolecular Science-Pure and Applied Chemistry, 2001. **38**(12): p. 1231-1243.
98. Boland, E.D., et al., *Utilizing acid pretreatment and electrospinning to improve biocompatibility of poly(glycolic acid) for tissue engineering.* Journal of Biomedical Materials Research Part B-Applied Biomaterials, 2004. **71B**(1): p. 144-152.
99. Subramanian, C., et al., *The melt electrospinning of polycaprolactone (PCL) ultrafine fibers.* Polymer-Based Smart Materials - Processes, Properties and Application, 2009. **1134**: p. 229-234.
100. Liu, W., et al., *Bead-line type PCL nanofibers from gelation electrospinning.* 2008 International Symposium on Fiber Based Scaffolds for Tissue Engineering, Proceedings, 2008: p. 56-59.
101. Romeo, V., et al., *Encapsulation and exfoliation of inorganic lamellar fillers into polycaprolactone by electrospinning.* Biomacromolecules, 2007. **8**(10): p. 3147-52.
102. Thomas, V., et al., *PCL/HA Nanocomposite fibers by electrospinning: structure-property relationship.* Abstracts of Papers of the American Chemical Society, 2006. **231**: p. -.
103. Thomas, V., et al., *Mechano-morphological studies of aligned nanofibrous scaffolds of polycaprolactone fabricated by electrospinning.* J Biomater Sci Polym Ed, 2006. **17**(9): p. 969-84.
104. Saraf, A., et al., *Regulated non-viral gene delivery from coaxial electrospun fiber mesh scaffolds.* Journal of Controlled Release, 2010. **143**(1): p. 95-103.
105. Chew, S.Y., et al., *Sustained release of proteins from electrospun biodegradable fibers.* Biomacromolecules, 2005. **6**(4): p. 2017-2024.
106. Chew, S.Y., et al., *Aligned Protein-Polymer Composite Fibers Enhance Nerve Regeneration: A Potential Tissue-Engineering Platform.* Adv Funct Mater, 2007. **17**(8): p. 1288-1296.
107. Chua, K.N., et al., *Stable immobilization of rat hepatocyte spheroids on galactosylated nanofiber scaffold.* Biomaterials, 2005. **26**(15): p. 2537-2547.

108. Spasova, M., et al., *Preparation of PLIA/PEG nanofibers by electrospinning and potential applications.* Journal of Bioactive and Compatible Polymers, 2007. **22**(1): p. 62-76.
109. Ko, H. and J. Kameoka, *Photo-crosslinked porous PEG hydrogel membrane via electrospinning.* Journal of Photopolymer Science and Technology, 2006. **19**(3): p. 413-418.
110. Wan, Y.Q., et al., *Electrospinning of high-molecule PEO solution.* Journal of Applied Polymer Science, 2007. **103**(6): p. 3840-3843.
111. Kakade, M., et al., *Alignment and molecular orientation in polyethylene oxide (PEO) nanofibers via Electrospinning.* Abstracts of Papers of the American Chemical Society, 2006. **231**: p. -.
112. Bender, J.D., et al., *Electrospinning of a polymeric ceramic precursor in the preparation of boron carbide nanofibers.* Abstracts of Papers of the American Chemical Society, 2004. **228**: p. U896-U896.
113. Li, D., J.T. McCann, and Y.N. Xia, *Electrospinning: A simple and versatile technique for producing ceramic nanofibers and nanotubes.* Journal of the American Ceramic Society, 2006. **89**(6): p. 1861-1869.
114. Li, D., Y.L. Wang, and Y.N. Xia, *Electrospinning of polymeric and ceramic nanofibers as uniaxially aligned arrays.* Nano Letters, 2003. **3**(8): p. 1167-1171.
115. Li, D. and Y.N. Xia, *Fabrication of ceramic and composite nanofibers by electrospinning.* Abstracts of Papers of the American Chemical Society, 2003. **226**: p. U425-U425.
116. Li, D. and Y.N. Xia, *Direct fabrication of composite and ceramic hollow nanofibers by electrospinning.* Nano Letters, 2004. **4**(5): p. 933-938.
117. Ayutsede, J., et al., *Carbon nanotube reinforced Bombyx mori silk nanofibers by the electrospinning process.* Biomacromolecules, 2006. **7**(1): p. 208-214.
118. Lala, N.L., V. Thavasi, and S. Ramakrishna, *Preparation of Surface Adsorbed and Impregnated Multi-walled Carbon Nanotube/Nylon-6 Nanofiber Composites and Investigation of their Gas Sensing Ability.* Sensors, 2009. **9**(1): p. 86-101.
119. Lam, H., et al., *Electrospinning of carbon nanotube reinforced nanocomposite fibrils and yarns.* Mechanical Properties of Nanostructured Materials and Nanocomposites, 2004. **791**: p. 353-358.
120. Sundaray, B., V. Subramanian, and T.S. Natarajan, *Preparation and characterization of polystyrene-multiwalled carbon nanotube composite fibers by electrospinning.* Journal of Nanoscience and Nanotechnology, 2007. **7**(6): p. 1793-1795.
121. Sun, Z., Zussman, E., Yarin, A., Wendorff, J. and Greiner, A, *Compound Core–Shell Polymer Nanofibers by Co-Electrospinning.* Advanced Materials, 2003. **15**(22): p. 1929.
122. Moghe, A.K. and B.S. Gupta, *Co-axial electrospinning for nanofiber structures: Preparation and applications.* Polymer Reviews, 2008. **48**(2): p. 353-377.
123. McCann, J.T., D. Li, and Y.N. Xia, *Electrospinning of nanofibers with core-sheath, hollow, or porous structures.* Journal of Materials Chemistry, 2005. **15**(7): p. 735-738.
124. Yu, J.H.F., Sergey V.; Rutledge, Gregory C., *Production of submicrometer diameter fibers by two-fluid electrospinning* Advanced Materials, 2004. **16**(17): p. 1562-1566.

125. Kurban, Z., et al., *A solution selection model for coaxial electrospinning and its application to nanostructured hydrogen storage materials.* Journal of Physical Chemistry C, 2010. **114**(49): p. 21201-21213.
126. Zhao, P., et al., *Biodegradable fibrous scaffolds composed of gelatin coated poly(epsilon-caprolactone) prepared by coaxial electrospinning.* J Biomed Mater Res A, 2007. **83**(2): p. 372-82.
127. Zhang, Y.Z., et al., *Characterization of the surface biocompatibility of the electrospun PCL-collagen nanofibers using fibroblasts.* Biomacromolecules, 2005. **6**(5): p. 2583-9.
128. Lu, Y., et al., *Mild immobilization of diverse macromolecular bioactive agents onto multifunctional fibrous membranes prepared by coaxial electrospinning.* Acta Biomater, 2009. **5**(5): p. 1562-74.
129. He, C.L., et al., *Coaxial electrospun poly(L-lactic acid) ultrafine fibers for sustained drug delivery.* Journal of Macromolecular Science, Part B: Physics, 2006. **45 B**(4): p. 515-524.
130. Li, H., et al., *Controlled release of PDGF-bb by coaxial electrospun dextran/poly(L- lactide-co-Œµ-caprolactone) fibers with an ultrafine core/shell structure.* Journal of Biomaterials Science, Polymer Edition, 2010. **21**(6-7): p. 803-819.
131. Wang, J.G., et al., *Preparation of coaxial electrospinning nanofibers for nerve growth factor delivery.* Journal of Clinical Rehabilitative Tissue Engineering Research, 2008. **12**(23): p. 4440-4444.
132. Zhang, Y.Z., et al., *Coaxial electrospinning of (fluorescein isothiocyanate-conjugated bovine serum albumin)-encapsulated poly(Œµ-caprolactone) nanofibers for sustained release.* Biomacromolecules, 2006. **7**(4): p. 1049-1057.
133. Jiang, H.L., et al., *A facile technique to prepare biodegradable coaxial electrospun nanofibers for controlled release of bioactive agents.* Journal of Controlled Release, 2005. **108**(2-3): p. 237-243.
134. Huang, H.H., et al., *Preparation of core-shell biodegradable microfibers for long-term drug delivery.* Journal of Biomedical Materials Research - Part A, 2009. **90**(4): p. 1243-1251.
135. Townsend-Nicholson, A. and S.N. Jayasinghe, *Cell electrospinning: a unique biotechnique for encapsulating living organisms for generating active biological microthreads/scaffolds.* Biomacromolecules, 2006. **7**(12): p. 3364-9.
136. Jayasinghe, S.N., S. Irvine, and J.R. McEwan, *Cell electrospinning highly concentrated cellular suspensions containing primary living organisms into cell-bearing threads and scaffolds.* Nanomedicine (Lond), 2007. **2**(4): p. 555-67.
137. Klein, S., Kuhn, J., Avrahami, R., Tarre, S., Beliavski, M., Green, M., Zussman, E., *Encapsulation of bacterial cells in electrospun microtubes* Biomacromolecules, 2009. **10**(7): p. 1751-1756.
138. Liao, I.C., et al., *Sustained viral gene delivery through core-shell fibers.* Journal of Controlled Release, 2009. **139**(1): p. 48-55.
139. Yang, Y., et al., *Core-sheath structured fibers with pDNA polyplex loadings for the optimal release profile and transfection efficiency as potential tissue engineering scaffolds.* Acta Biomaterialia, 2011. **7**(6): p. 2533-43.
140. Liao, I.C., S.Y. Chew, and K.W. Leong, *Aligned core-shell nanofibers delivering bioactive proteins.* Nanomedicine, 2006. **1**(4): p. 465-471.

141. Yan, S., et al., *Poly(l-lactide-co-Œµ-caprolactone) electrospun nanofibers for encapsulating and sustained releasing proteins.* Polymer, 2009. **50**(17): p. 4212-4219.
142. Yang, D.Z., Y.H. Long, and J. Nie, *Release of lysozyme from electrospun PVA/lysozyme-gelatin scaffolds.* Frontiers of Materials Science in China, 2008. **2**(3): p. 261-265.
143. Chen, P., et al., *A controlled release system of superoxide dismutase by electrospun fiber and its antioxidant activity in vitro.* Journal of Materials Science: Materials in Medicine, 2010. **21**(2): p. 609-614.
144. Li, X., et al., *Encapsulation of proteinase K in PELA ultrafine fibers by emulsion electrospinning: preparation and in vitro evaluation.* Colloid and Polymer Science, 2010: p. 1-7.
145. Dai, Y., et al., *In situ encapsulation of laccase in microfibers by emulsion electrospinning: Preparation, characterization, and application.* Bioresource Technology, 2010. **101**(23): p. 8942-8947.
146. Zhang, J., et al., *Co-electrospun fibrous scaffold-adsorbed DNA for substrate-mediated gene delivery.* Journal of biomedical materials research. Part A, 2011. **96**(1): p. 212-20.
147. Qiu, X.F., et al., *[Controlled release of siRNA nanoparticles loaded in a novel external stent prepared by emulsion electrospinning attenuates neointima hyperplasia in vein grafts]*. Zhonghua yi xue za zhi, 2009. **89**(41): p. 2938-42.
148. Cao, H., et al., *RNA interference by nanofiber-based siRNA delivery system.* Journal of controlled release : official journal of the Controlled Release Society, 2010. **144**(2): p. 203-12.
149. Rujitanaroj, P.O., et al., *Nanofiber-mediated controlled release of siRNA complexes for long term gene-silencing applications.* Biomaterials, 2011. **32**(25): p. 5915-23.
150. Xie, J. and C.H. Wang, *Electrospun micro- and nanofibers for sustained delivery of paclitaxel to treat C6 glioma in vitro.* Pharmaceutical Research, 2006. **23**(8): p. 1817-1826.
151. Wang, H., et al., *Release of ibuprofen from PEG-PLLA electrospun fibers containing poly(ethylene glycol)-b-poly(Œ±-hydroxy octanoic acid) as an additive.* Chinese Journal of Polymer Science (English Edition), 2010. **28**(3): p. 417-425.
152. Kenawy, E.R., et al., *Controlled release of ketoprofen from electrospun poly(vinyl alcohol) nanofibers.* Materials Science and Engineering A, 2007. **459**(1-2): p. 390-396.
153. Xu, X., et al., *The release behavior of doxorubicin hydrochloride from medicated fibers prepared by emulsion-electrospinning.* European Journal of Pharmaceutics and Biopharmaceutics, 2008. **70**(1): p. 165-170.
154. Taepaiboon, P., U. Rungsardthong, and P. Supaphol, *Vitamin-loaded electrospun cellulose acetate nanofiber mats as transdermal and dermal therapeutic agents of vitamin A acid and vitamin E.* European journal of pharmaceutics and biopharmaceutics : official journal of Arbeitsgemeinschaft fur Pharmazeutische Verfahrenstechnik e.V, 2007. **67**(2): p. 387-97.
155. Buschle-Diller, G., et al., *Release of antibiotics from electrospun bicomponent fibers.* Cellulose, 2007. **14**(6): p. 553-562.
156. Dheraprasart, C., et al., *Morphology, release characteristics, and antimicrobial effect of nisin-loaded electrospun gelatin fiber mat.* Journal of Food Protection, 2009. **72**(11): p. 2293-2300.

157. Brewster, M.E., et al., *The use of polymer-based electrospun nanofibers containing amorphous drug dispersions for the delivery of poorly water-soluble pharmaceuticals.* Pharmazie, 2004. **59**(5): p. 387-391.
158. Luong-Van, E., et al., *Controlled release of heparin from poly(Œµ-caprolactone) electrospun fibers.* Biomaterials, 2006. **27**(9): p. 2042-2050.
159. Maretschek, S., A. Greiner, and T. Kissel, *Electrospun biodegradable nanofiber nonwovens for controlled release of proteins.* Journal of Controlled Release, 2008. **127**(2): p. 180-187.
160. Li, X., et al., *Distribution of Sorbitan Monooleate in poly(l-lactide-co-Œµ-caprolactone) nanofibers from emulsion electrospinning.* Colloids and Surfaces B: Biointerfaces, 2009. **69**(2): p. 221-224.
161. Erisken, C., D.M. Kalyon, and H. Wang, *Viscoelastic and biomechanical properties of osteochondral tissue constructs generated from graded polycaprolactone and beta-tricalcium phosphate composites.* J Biomech Eng, 2010. **132**(9): p. 091013.
162. Erisken, C., D.M. Kalyon, and H. Wang, *Functionally graded electrospun polycaprolactone and beta-tricalcium phosphate nanocomposites for tissue engineering applications.* Biomaterials, 2008. **29**(30): p. 4065-73.
163. Angeles, M., H.L. Cheng, and S.S. Velankar, *Emulsion electrospinning: Composite fibers from drop breakup during electrospinning.* Polymers for Advanced Technologies, 2008. **19**(7): p. 728-733.
164. Shastri, V.P., J.C. Sy, and A.S. Klemm, *Emulsion as a means of controlling electrospinning of polymers.* Advanced Materials, 2009. **21**(18): p. 1814-1819.
165. Xiaoran Li, J.X., Xiaoyan Yuan and Younan Xia, *Coating Electrospun Poly(ε -caprolactone) Fibers with Gelatin and Calcium Phosphate and Their Use as Biomimetic Scaffolds for Bone Tissue Engineering.* Langmuir, 2008. **24**(24): p. 14145-14150.
166. Natu, M.V., H.C. de Sousa, and M.H. Gil, *Effects of drug solubility, state and loading on controlled release in bicomponent electrospun fibers.* Int J Pharm, 2010. **397**(1-2): p. 50-8.
167. Gandhi, M., et al., *Mechanistic Examination of Protein Release from Polymer Nanofibers.* Mol Pharm, 2009.
168. Wang, B.C., et al., *Applications of Electrospinning Technique in Drug Delivery.* Chemical Engineering Communications, 2010. **197**(10): p. 1315-1338.
169. Handarmin, G.J.Y.T., S Bibekananda, G T Marcy, E L K Goh and S Y Chew, *Nanofibrous scaffold with incorporated protein gradient for directing neurite outgrowth.* Drug Delivery and Translational Research, 2011. **1**(2): p. 147-160.
170. Chow, W.N., et al., *Evaluating neuronal and glial growth on electrospun polarized matrices: bridging the gap in percussive spinal cord injuries.* Neuron Glia Biol, 2007. **3**(2): p. 119-126.
171. Corey, J.M., et al., *Aligned electrospun nanofibers specify the direction of dorsal root ganglia neurite growth.* J Biomed Mater Res A, 2007. **83**(3): p. 636-45.
172. Schnell, E., et al., *Guidance of glial cell migration and axonal growth on electrospun nanofibers of poly-epsilon-caprolactone and a collagen/poly-epsilon-caprolactone blend.* Biomaterials, 2007. **28**(19): p. 3012-25.
173. Panseri, S., et al., *Electrospun micro- and nanofiber tubes for functional nervous regeneration in sciatic nerve transections.* BMC Biotechnol, 2008. **8**: p. 39.

174. Yao, L., et al., *Orienting neurite growth in electrospun fibrous neural conduits.* J Biomed Mater Res B Appl Biomater, 2009. **90**(2): p. 483-91.
175. Corey, J.M., et al., *Aligned electrospun nanofibers specify the direction of dorsal root ganglia neurite growth.* Journal of Biomedical Materials Research - Part A, 2007. **83**(3): p. 636-645.
176. Lee, J.Y., et al., *Enhanced polarization of embryonic hippocampal neurons on micron scale electrospun fibers.* Journal of Biomedical Materials Research Part A, 2010. **92A**(4): p. 1398-1406.
177. Griffin, J., et al., *Salicylic acid-derived poly(anhydride-ester) electrospun fibers designed for regenerating the peripheral nervous system.* Journal of biomedical materials research. Part A, 2011. **97**(3): p. 230-42.
178. Cho, Y.I., et al., *Nerve growth factor (NGF)-conjugated electrospun nanostructures with topographical cues for neuronal differentiation of mesenchymal stem cells.* Acta Biomaterialia, 2010. **6**(12): p. 4725-4733.
179. Christopherson, G.T., H. Song, and H.Q. Mao, *The influence of fiber diameter of electrospun substrates on neural stem cell differentiation and proliferation.* Biomaterials, 2009. **30**(4): p. 556-564.
180. Chew, S.Y., et al., *The effect of the alignment of electrospun fibrous scaffolds on Schwann cell maturation.* Biomaterials, 2008. **29**(6): p. 653-61.
181. Wang, H.B., et al., *Varying the diameter of aligned electrospun fibers alters neurite outgrowth and Schwann cell migration.* Acta Biomater, 2010. **6**(8): p. 2970-8.
182. Schnell, E., et al., *Guidance of glial cell migration and axonal growth on electrospun nanofibers of poly-Œµ-caprolactone and a collagen/poly-Œµ-caprolactone blend.* Biomaterials, 2007. **28**(19): p. 3012-3025.
183. Kim, Y.t., et al., *The role of aligned polymer fiber-based constructs in the bridging of long peripheral nerve gaps.* Biomaterials, 2008. **29**(21): p. 3117-3127.
184. Gertz, C.C., et al., *Accelerated neuritogenesis and maturation of primary spinal motor neurons in response to nanofibers.* Developmental Neurobiology, 2010. **70**(8): p. 589-603.
185. Corey, J.M., et al., *The design of electrospun PLLA nanofiber scaffolds compatible with serum-free growth of primary motor and sensory neurons.* Acta Biomaterialia, 2008. **4**(4): p. 863-875.
186. Liu, X., et al., *Guidance of neurite outgrowth on aligned electrospun polypyrrole/ poly(styrene-Œ≤-isobutylene-Œ≤-styrene) fiber platforms.* Journal of Biomedical Materials Research - Part A, 2010. **94**(4): p. 1004-1011.
187. Xie, J., et al., *The differentiation of embryonic stem cells seeded on electrospun nanofibers into neural lineages.* Biomaterials, 2009. **30**(3): p. 354-362.
188. Ratanavaraporn, J., et al., *Influences of physical and chemical crosslinking techniques on electrospun type A and B gelatin fiber mats.* International Journal of Biological Macromolecules, 2010. **47**(4): p. 431-438.
189. Sisson, K., et al., *Evaluation of cross-linking methods for electrospun gelatin on cell growth and viability.* Biomacromolecules, 2009. **10**(7): p. 1675-1680.
190. Qian, Y.F., et al., *Cross-linking of gelatin and chitosan complex nanofibers for tissue-engineering scaffolds.* Journal of Biomaterials Science, Polymer Edition, 2011. **22**(8): p. 1099-1113.
191. Zhao, J., et al., *Crosslinking of electrospun fibrous gelatin scaffolds for apatite mineralization.* Journal of Applied Polymer Science, 2011. **119**(2): p. 786-793.

192. Panzavolta, S., et al., *Electrospun gelatin nanofibers: Optimization of genipin cross-linking to preserve fiber morphology after exposure to water.* Acta Biomaterialia, 2011. **7**(4): p. 1702-1709.
193. Liu, S., Y. Su, and Y. Chen, *Fabrication, surface properties and protein encapsulation/release studies of electrospun gelatin nanofibers.* Journal of Biomaterials Science, Polymer Edition, 2011. **22**(7): p. 945-955.
194. Sisson, K., et al., *Fiber diameters control osteoblastic cell migration and differentiation in electrospun gelatin.* Journal of Biomedical Materials Research - Part A, 2010. **94**(4): p. 1312-1320.
195. Ko, J.H., et al., *Characterization of cross-linked gelatin nanofibers through electrospinning.* Macromolecular Research, 2010. **18**(2): p. 137-143.
196. Khor, E., *Methods for the treatment of collagenous tissues for bioprostheses.* Biomaterials, 1997. **18**(2): p. 95-105.
197. Moshnikova, A.B., et al., *Cytotoxic activity of 1-ethyl-3-(3-dimethylaminopropyl)-carbodiimide is underlain by DNA interchain cross-linking.* Cellular and Molecular Life Sciences, 2006. **63**(2): p. 229-234.
198. Usui, T., et al., *Cytotoxicity and oxidative stress induced by the glyceraldehyde-related maillard reaction products for HL-60 cells.* Bioscience, Biotechnology and Biochemistry, 2004. **68**(2): p. 333-340.
199. Yamagishi, S.I., et al., *Advanced glycation end products-induced apoptosis and overexpression of vascular endothelial growth factor in bovine retinal pericytes.* Biochemical and Biophysical Research Communications, 2002. **290**(3): p. 973-978.
200. Usui, T. and F. Hayase, *Isolation and identification of the 3-hydroxy-5-hydroxymethyl-pyridinium compound as a novel advanced glycation end product on glyceraldehyde-related maillard reaction.* Bioscience, Biotechnology and Biochemistry, 2003. **67**(4): p. 930-932.
201. Tietze, F., *Enzymic method for quantitative determination of nanogram amounts of total and oxidized glutathione: Applications to mammalian blood and other tissues.* Analytical Biochemistry, 1969. **27**(3): p. 502-522.
202. Yokoyama, K., N. Nio, and Y. Kikuchi, *Properties and applications of microbial transglutaminase.* Applied Microbiology and Biotechnology, 2004. **64**(4): p. 447-454.
203. Hornyak, T.J., P.D. Bishop, and J.A. Shafer, *Œ±-Thrombin-catalyzed activation of human platelet factor XIII: Relationship between proteolysis and factor XIIIa activity.* Biochemistry, 1989. **28**(18): p. 7326-7332.
204. Chung, S.I., M.S. Lewis, and J.E. Folk, *Relationships of the catalytic properties of human plasma and platelet transglutaminases (activated blood coagulation factor XIII) to their subunit structures.* Journal of Biological Chemistry, 1974. **249**(3): p. 940-950.
205. Aeschlimann, D. and M. Paulsson, *Transglutaminases: Protein cross-linking enzymes in tissues and body fluids.* Thrombosis and Haemostasis, 1994. **71**(4): p. 402-415.
206. Fesus, L., P.J.A. Davies, and M. Piacentini, *Apoptosis: Molecular mechanisms in programmed cell death.* European Journal of Cell Biology, 1991. **56**(2): p. 170-177.
207. Shanmugasundaram, S., et al., *Tissue transglutaminase regulates chondrogenesis in mesenchymal stem cells on collagen type XI matrices.* Amino Acids, 2011: p. 1-9.

208. Tseng, C.S. and H.M. Lai, *Physicochemical properties of wheat flour dough modified by microbial transglutaminase.* Journal of Food Science, 2002. **67**(2): p. 750-755.
209. Tsukamasa, Y., et al., *Total activity of transglutaminase at various temperatures in several fish meats.* Fisheries Science, 2002. **68**(4): p. 929-933.
210. Kanaji, T., et al., *Primary structure of microbial transglutaminase from Streptoverticillium sp. strain s-8112.* Journal of Biological Chemistry, 1993. **268**(16): p. 11565-11572.
211. Tagami, U., et al., *Substrate specificity of microbial transglutaminase as revealed by three-dimensional docking simulation and mutagenesis.* Protein Engineering, Design and Selection, 2009. **22**(12): p. 747-752.
212. Taguchi, S., et al., *Substrate specificity analysis of microbial transglutaminase using proteinaceous protease inhibitors as natural model substrates.* Journal of Biochemistry, 2000. **128**(3): p. 415-425.
213. Bernard, B.K., S. Tsubuku, and S. Shioya, *Acute toxicitiy and genotoxicity studies of a microbial transglutaminase.* International Journal of Toxicology, 1998. **17**(6): p. 703-721.
214. Broderick, E.P., et al., *Enzymatic stabilization of gelatin-based scaffolds.* Journal of Biomedical Materials Research - Part B Applied Biomaterials, 2005. **72**(1): p. 37-42.
215. Yung, C.W., W.E. Bentley, and T.A. Barbari, *Diffusion of interleukin-2 from cells overlaid with cytocompatible enzyme-crosslinked gelatin hydrogels.* Journal of Biomedical Materials Research Part A, 2010. **95A**(1): p. 25-32.
216. Bandiera, A., *Transglutaminase-catalyzed preparation of human elastin-like polypeptide-based three-dimensional matrices for cell encapsulation.* Enzyme and Microbial Technology, 2011.
217. Yao, L., et al., *The effect of laminin peptide gradient in enzymatically cross-linked collagen scaffolds on neurite growth.* Journal of Biomedical Materials Research - Part A, 2010. **92**(2): p. 484-492.
218. Ciardelli, G., et al., *Enzymatically crosslinked porous composite matrices for bone tissue regeneration.* Journal of Biomedical Materials Research - Part A, 2010. **92**(1): p. 137-151.
219. Garcia, Y., et al., *Assessment of cell viability in a three-dimensional enzymatically cross-linked collagen scaffold.* Journal of Materials Science: Materials in Medicine, 2007. **18**(10): p. 1991-2001.
220. Torres-Giner, S., et al., *Comparative performance of electrospun collagen nanofibers cross-linked by means of different methods.* Acs Applied Materials & Interfaces, 2009. **1**(1): p. 218-223.
221. Chen, T., et al., *Enzymatic methods for in situ cell entrapment and cell release.* Biomacromolecules, 2003. **4**(6): p. 1558-1563.
222. Liu, Y., et al., *Biomimetic sealant based on gelatin and microbial transglutaminase: An initial in vivo investigation.* Journal of Biomedical Materials Research - Part B Applied Biomaterials, 2009. **91**(1): p. 5-16.
223. Yung, C.W., et al., *Transglutaminase crosslinked gelatin as a tissue engineering scaffold.* Journal of Biomedical Materials Research - Part A, 2007. **83**(4): p. 1039-1046.
224. Kuwahara, K., et al., *Cell delivery using an injectable and adhesive transglutaminase-gelatin gel.* Tissue Engineering - Part C: Methods, 2010. **16**(4): p. 609-618.

225. Ruoslahti, E., *RGD AND OTHER RECOGNITION SEQUENCES FOR INTEGRINS.* Annual Review of Cell and Developmental Biology, 1996. **12**(1): p. 697-715.
226. Eastoe, J.E., *The amino acid composition of mammalian collagen and gelatin.* The Biochemical journal, 1955. **61**(4): p. 589-600.
227. Elliott, J.T., et al., *Thin Films of Collagen Affect Smooth Muscle Cell Morphology,Ä†.* Langmuir, 2002. **19**(5): p. 1506-1514.
228. Motoki, M. and K. Seguro, *Transglutaminase and its use for food processing.* Trends in Food Science and Technology, 1998. **9**(5): p. 204-210.
229. Cui, L., et al., *Stability and conformational changes of transglutaminase from Streptomyces hygroscopicus in ethanol-aqueous medium.* Process Biochemistry, 2008. **43**(8): p. 887-891.
230. Kutemeyer, C., et al., *The influence of salts and temperature on enzymatic activity of microbial transglutaminase.* Food Control, 2005. **16**(8): p. 735-737.
231. Maniwa, S., et al., *Effects of neurotrophic factors on chemokinesis of Schwann cells in culture.* Scandinavian Journal of Plastic and Reconstructive Surgery and Hand Surgery, 2003. **37**(1): p. 14-7.
232. De Simone, R., Ambrosini, E., Carnevale, D., Ajmone-Cat, M.A., Minghetti, L., *NGF promotes microglial migration through the activation of its high affinity receptor: Modulation by TGF-β* Journal of Neuroimmunology, 2007. **190** (1-2): p. 53-60.
233. Jin Y. Kim, X.X., Eduardo K. Moioli, Jenny Chung, Chang Hun Lee, Mo Chen, Susan Y. Fu, Peter D. Koch, Jeremy J. Mao., *Regeneration of dental-pulp-like tissue by chemotaxis-induced cell homing* Tissue Eng Part A, 2010. **16**(10): p. 3023-3031.
234. Yamamoto, N., A. Tamada, and F. Murakami, *Wiring of the brain by a range of guidance cues.* Progress in Neurobiology, 2002. **68**(6): p. 393-407.
235. Dickson, B.J., *Molecular mechanisms of axon guidance.* Science, 2002. **298**(5600): p. 1959-64.
236. Kapur, T.A. and M.S. Shoichet, *Chemically-bound nerve growth factor for neural tissue engineering applications.* J Biomater Sci Polym Ed, 2003. **14**(4): p. 383-94.
237. William J Rosoff, J.S.U., Mark A Esrick, Ryan G McAllister, Linda J Richards & Geoffrey J Goodhill, *A new chemotaxis assay shows the extreme sensitivity of axons to molecular gradients.* Nature Neuroscience, 2004. **7**: p. 678-682.
238. Sano, M. and M. Iwanaga, *Local sprouting of neurites from cultured PC12D cells in response to a concentration gradient of nerve growth factor.* Brain Research, 1994. **656**(1): p. 210-4.
239. Kim, D., et al., *Selective and tunable gradient device for cell culture and chemotaxis study.* Lab Chip, 2009. **9**(12): p. 1797-800.
240. Barkefors, I., et al., *A fluidic device to study directional angiogenesis in complex tissue and organ culture models.* Lab Chip, 2009. **9**(4): p. 529-35.
241. Nakashima, Y., Yasuda, T. , *Cell differentiation guidance using chemical stimulation controlled by a microfluidic device.* Sensors and Actuators, A: Physical, 2007. **139**(1-2): p. 252-258.
242. Wang, X.W., E.; Zhang, X.; Meinel, L.; Vunjak-Novakovic, G.; Kaplan, D.L., *Growth factor gradients via microsphere delivery in biopolymer scaffolds for osteochondral tissue engineering.* Journal of Controlled Release, 2009. **134**: p. 81-90.

243. Peret, B.J. and W.L. Murphy, *Controllable Soluble Protein Concentration Gradients in Hydrogel Networks.* Adv Funct Mater, 2008. **18**(21): p. 3410-3417.
244. Ayutsede, J., F.K. Ko, and M. Gandhi, *Carbon nanotube reinforced Bombyx Mori nanofibers by the electrospinning process.* Abstracts of Papers of the American Chemical Society, 2004. **228**: p. U514-U514.
245. Moroni, L., et al., *Fiber diameter and texture of electrospun PEOT/PBT scaffolds influence human mesenchymal stem cell proliferation and morphology, and the release of incorporated compounds.* Biomaterials, 2006. **27**(28): p. 4911-22.
246. Bashur, C.A., et al., *Effect of fiber diameter and alignment of electrospun polyurethane meshes on mesenchymal progenitor cells.* Tissue Eng Part A, 2009. **15**(9): p. 2435-45.
247. Jiang, X., et al., *Current applications and future perspectives of artificial nerve conduits.* Experimental Neurology, 2010. **223**(1): p. 86-101.
248. DiPaolo, B.C. and K.A. Moxon. *Nanofiber scaffolding for improved neural electrode biocompatibility*. 2003.
249. DiPaolo, B.C., et al. *Nanoscale surface modification of thin film microelectrodes to improve biocompatibility*. 2002.
250. Abidian, M.R. and D.C. Martin, *Multifunctional nanobiomaterials for neural interfaces.* Advanced Functional Materials, 2009. **19**(4): p. 573-585.
251. Li, X., et al., *Encapsulation of proteins in poly(l-lactide-co-caprolactone) fibers by emulsion electrospinning.* Colloids and Surfaces B: Biointerfaces, 2010. **75**(2): p. 418-424.
252. Zhang, Y.Z., et al., *Coaxial electrospinning of (fluorescein isothiocyanate-conjugated bovine serum albumin)-encapsulated poly(epsilon-caprolactone) nanofibers for sustained release.* Biomacromolecules, 2006. **7**(4): p. 1049-57.
253. Su, Y., et al., *Fabrication and characterization of biodegradable nanofibrous mats by mix and coaxial electrospinning.* Journal of Materials Science: Materials in Medicine, 2009. **20**(11): p. 2285-2294.
254. Sisson, K., et al., *Fiber diameters control osteoblastic cell migration and differentiation in electrospun gelatin.* J Biomed Mater Res A, 2010. **94**(4): p. 1312-20.
255. Stach, R.W., N. Garian, and E.J. Olender, *Biological activity of the Œ≤ nerve growth factor: The effects of various added proteins.* Journal of Neurochemistry, 1979. **33**(1): p. 257-261.
256. Katzir, I., et al., *A quantitative bioassay for nerve growth factor, using PC12 clones expressing different levels of trkA receptors.* Journal of Molecular Neuroscience, 2002. **18**(3): p. 251-264.
257. Pean, J.M., et al., *NGF release from poly(D,L-lactide-co-glycolide) microspheres. Effect of some formulation parameters on encapsulated NGF stability.* Journal of Controlled Release, 1998. **56**(1-3): p. 175-187.
258. Rukenstein, A. and L.A. Greene, *The quantitative bioassay of nerve growth factor: Use of frozen 'primed' PC12 pheochromocytoma cells.* Brain Research, 1983. **263**(1): p. 177-180.
259. Das, K.P., T.M. Freudenrich, and W.R. Mundy, *Assessment of PC12 cell differentiation and neurite growth: A comparison of morphological and neurochemical measures.* Neurotoxicology and Teratology, 2004. **26**(3): p. 397-406.

260. Chang, C.J., *Effects of nerve growth factor from genipin-crosslinked gelatin in polycaprolactone conduit on peripheral nerve regeneration - In vitro and in vivo.* Journal of Biomedical Materials Research - Part A, 2009. **91**(2): p. 586-596.
261. Geldof, A.A., *Nerve-growth-factor dependent neurite outgrowth assay; a research model for chemotherapy-induced neuropathy.* Journal of Cancer Research and Clinical Oncology, 1995. **121**(11): p. 657-660.
262. Seeley, P.J., et al., *Differential inhibition of nerve growth factor and epidermal growth factor effects on the PC12 pheochromocytoma line.* Journal of Cell Biology, 1984. **98**(2): p. 417-426.
263. Shin, H.J., et al., *Electrospun PLGA nanofiber scaffolds for articular cartilage reconstruction: mechanical stability, degradation and cellular responses under mechanical stimulation in vitro.* Journal of Biomaterials Science-Polymer Edition, 2006. **17**(1-2): p. 103-119.
264. Yoshimoto, H., et al., *A biodegradable nanofiber scaffold by electrospinning and its potential for bone tissue engineering.* Biomaterials, 2003. **24**(12): p. 2077-2082.
265. Cao, H.Q., et al., *The topographical effect of electrospun nanofibrous scaffolds on the in vivo and in vitro foreign body reaction.* Journal of Biomedical Materials Research Part A, 2010. **93A**(3): p. 1151-1159.
266. Leong, M.F., et al., *Fabrication and in vitro and in vivo cell infiltration study of a bilayered cryogenic electrospun poly(D,L-lactide) scaffold.* J Biomed Mater Res A, 2010. **94**(4): p. 1141-9.
267. Leong, M.F., et al., *In vitro cell infiltration and in vivo cell infiltration and vascularization in a fibrous, highly porous poly(D,L-lactide) scaffold fabricated by cryogenic electrospinning technique.* J Biomed Mater Res A, 2009. **91**(1): p. 231-40.